Development 140, 3645-3656 (2013) doi:10.1242/dev.095596


# Post-transcriptional regulation of myotube elongation and myogenesis by Hoi Polloi

**Aaron N. Johnson[1,2,*], Maysa H. Mokalled[3], Juliana M. Valera[2], Kenneth D. Poss[3] and Eric N. Olson[1,*]**

## SUMMARY

Striated muscle development requires the coordinated expression of genes involved in sarcomere formation and contractility, as well as genes that determine muscle morphology. However, relatively little is known about the molecular mechanisms that control the early stages of muscle morphogenesis. To explore this facet of myogenesis, we performed a genetic screen for regulators of somatic muscle morphology in *Drosophila*, and identified the putative RNA-binding protein (RBP) Hoi Polloi (Hoip). Hoip is expressed in striated muscle precursors within the muscle lineage and controls two genetically separable events: myotube elongation and sarcomeric protein expression. Myotubes fail to elongate in *hoip* mutant embryos, even though the known regulators of somatic muscle elongation, target recognition and muscle attachment are expressed normally. In addition, a majority of sarcomeric proteins, including Myosin Heavy Chain (MHC) and Tropomyosin, require Hoip for their expression. A transgenic *MHC* construct that contains the endogenous *MHC* promoter and a spliced open reading frame rescues MHC protein expression in *hoip* embryos, demonstrating the involvement of Hoip in pre-mRNA splicing, but not in transcription, of muscle structural genes. In addition, the human Hoip ortholog NHP2L1 rescues muscle defects in *hoip* embryos, and knockdown of endogenous *nhp2l1* in zebrafish disrupts skeletal muscle development. We conclude that Hoip is a conserved, post-transcriptional regulator of muscle morphogenesis and structural gene expression.

**KEY WORDS: Myotube elongation, Post-transcriptional regulation, Myogenesis, *Drosophila*, Zebrafish**

## INTRODUCTION

The transcriptional regulatory networks that direct muscle precursor cell specification and the expression of muscle structural genes have been well defined. However, the possible post-transcriptional contribution to mesoderm development is only beginning to come to light (Biedermann et al., 2010; Toledano-Katchalski et al., 2007; Yarnitzky et al., 1998). The unique properties of *Drosophila*, including external development and an extensive array of genetic tools, have allowed the discrete cellular processes directing muscle development to be dissected in detail (Guerin and Kramer, 2009a; Schejter and Baylies, 2010; Schnorrer and Dickson, 2004).

Embryonic somatic muscle development in *Drosophila* is a multistep process that initiates with the specification of founder cells from a field of myogenic competent cells in the mesoderm (Carmena et al., 1995; Jagla et al., 1998). Founder cells express a unique set of muscle identity genes, encoding transcription factors, that direct differentiation into one of 30 somatic muscles (de Joussineau et al., 2012). Once specified, muscle founders begin the process of migration and elongation that can be divided into three phases (Schnorrer and Dickson, 2004). During the first phase, founder cells migrate to their correct position within the segment. The second phase begins when the founder cells initiate myoblast fusion and form polarized myotubes that elongate along a single axis. The myotubes then form extensive filopodia in the direction of initial polarity, presumably in response to guidance cues from tendon cells in the overlying epidermis (Guerin and Kramer, 2009a; Schnorrer and Dickson, 2004). The center of the myotube remains localized while the ends of the myotube elongate towards their respective muscle-attachment sites (Schnorrer and Dickson, 2004). The final phase of elongation initiates when the myotube ends reach their muscle attachment sites and filopodia no longer form. The myotube then localizes integrin-mediated adhesion complexes with the overlying tendon cells to establish strong myotendinous junctions (Schejter and Baylies, 2010).

The mechanisms that control myotube elongation during somatic muscle morphogenesis are poorly understood. Slit is the single guidance molecule known to direct both myotube elongation and target site recognition, but loss of Slit modestly affects the elongation of only a subset of myotubes (Kramer et al., 2001). Nascent myotubes must undergo extensive cytoskeletal rearrangements during elongation, and recent work has focused on the role of microtubule dynamics in this process (Folker et al., 2012; Guerin and Kramer, 2009b). Tumbleweed (Tum) is a Rac family GTPase-activating protein that becomes localized to the nuclear periphery via its association with the microtubule-associated protein Pavarotti (Pav). Loss of *pav* or *tum* disrupts microtubule polarity and polarized growth, mislocalizes the minus-end microtubule nucleator γ-tubulin and causes modest myotube elongation defects (Guerin and Kramer, 2009b). A second regulator of microtubule dynamics, Dynein heavy chain (Dhc64C), is also required for myotube elongation but its role is restricted to the final stages of elongation (Folker et al., 2012). Although microtubule dynamics plays a key role in the process, the mechanisms that initiate myotube elongation and the downstream targets of intracellular messenger proteins, such as Tum, remain largely unknown.

The cellular events that regulate myotube morphology are distinct from the molecular processes that direct terminal differentiation and structural gene expression. Embryos defective in myoblast fusion express Myosin Heavy Chain (MHC) in unfused mononucleate

[1]Department of Molecular Biology, UT Southwestern Medical Center at Dallas, Dallas, TX 75390-9148, USA. [2]Department of Integrative Biology, University of Colorado Denver, Denver, CO 80204, USA. [3]Department of Cell Biology and Howard Hughes Medical Institute, Duke University Medical Center, Durham, NC 27710, USA.

*Authors for correspondence (aaron.n.johnson@ucdenver.edu; eric.olson@utsouthwestern.edu)

**Accepted 22 June 2013**

founder cells; this striking phenotype has been exploited in genetic screens to identify novel regulators of myoblast fusion (Chen and Olson, 2001). Components of the sarcomere, the basic unit of muscle contraction, are subject to extensive post-transcriptional regulation. For example, *Drosophila* MHC is encoded by a single genomic locus that can produce 480 unique protein isoforms (Zhang and Bernstein, 2001). These isoforms encode variant regions of the MHC globular head and provide diversity in contractile performance (Kronert et al., 1994). However, the RNA-binding proteins (RBPs) that regulate the production of different MHC isoforms have not been identified.

In a screen for genes that regulate somatic muscle morphology in *Drosophila*, we identified the putative RBP Hoi polloi (Hoip). *hoip* embryos show two dramatic phenotypes: myotube elongation does not initiate, even though founder cell specification and myoblast fusion initiate normally and striated muscles fail to express multiple sarcomeric proteins, including MHC and Tropomyosin (Tm). *hoip* expression is tissue specific and within the muscle lineage is restricted to striated muscle precursors. By RNA deep sequencing (RNA-seq), we found that known regulators of myotube elongation are expressed correctly in *hoip* mutant embryos, suggesting Hoip orchestrates a previously unrecognized post-transcriptional mechanism to initiate elongation. Functional rescue experiments demonstrate that Hoip directs pre-mRNA splicing during myogenesis. The human Hoip ortholog NHP2L1 can rescue the *hoip* phenotype in *Drosophila*, and morpholino (MO) knockdown experiments in zebrafish indicate that *nhp2l1* is a conserved essential regulator of myogenesis. This is the first study to show a tissue-specific role for Hoip or its orthologs *in vivo*, to identify a robust genetic block in the second phase of myotube elongation, and to address post-transcriptional regulation of sarcomeric gene expression by a putative RBP during *Drosophila* embryogenesis.

## MATERIALS AND METHODS

### *Drosophila* genetics

All stocks were obtained from the Bloomington Stock Center unless otherwise noted. The stocks used in this study were: *Df(2L)ED90, Df(2L)ED678, Df(2L)Exel6024, Df(2L)Exel7043, Df(2L)Exel7042, Df(2L)Exel8041, Df(2L)BSC216, Df(2L)BSC108, Df(3R)Exel6191, P{lacW}hoip$^{k07104}$*, *P{Mhc.EMB}* (Wells et al., 1996), *Mhc$^{1}$* (Wells et al., 1996), *P{Gal4-kirre$^{rP298}$}, P{kirre$^{rP298}$.lacZ}* (Nose et al., 1998) and the Baylor P-element Mapping Kit (Zhai et al., 2003). The *Cyo, P{Gal4-Twi}, P{2X-UAS.eGFP}*; *Cyo, P{wg.lacZ}*; and *TM3, P{ftz.lacZ}* balancers were used to identify homozygous embryos.

### EMS mutagenesis and gene mapping

Isogenic, starved *w$^{1118}$* males were fed 25 mM EMS in 1% sucrose overnight and mated *en masse* as shown (supplementary material Fig. S1A). Mapping of *hoip$^{1}$* was performed as described previously (Zhai et al., 2003).

### Immunohistochemistry, *in situ* hybridization and imaging

Antibodies used include anti-Mef2 (Lilly et al., 1995), anti-Nau (Wei et al., 2007), anti-Tin (Venkatesh et al., 2000), anti-MHC (Kiehart and Feghali, 1986), anti-Kr (Kosman et al., 1998), anti-MF20 (DSHB), anti-Tropomyosin (Abcam, MAC141), anti-GFP (Torrey Pines Laboratories), anti-βPS (DSHB), anti-Talin (DSHB), anti-22C10 (DSHB) and anti-βgal (Promega). Alexa488-, Alexa633- and HRP-conjugated secondary antibodies in conjunction with the TSA system (Molecular Probes) were used to detect primary antibodies. Antibody staining and *in situ* hybridization was performed as described (Johnson et al., 2007). Mef2 was directly conjugated with Zenon633 (Molecular Probes) for co-labeling with rabbit primary antibodies. The following templates were used to generate *in situ* probes: RE51843 (*hoip*; DGRC) and *Mhc.Exon4-6* (a gift from S. Bernstein, SDSU, San Diego, CA, USA). Images were generated with LSM510 and LSM710 confocal microscopes. Control and mutant embryos were prepared and imaged in parallel.

### RT-PCR

Appropriately aged embryos were dechorionated (*Drosophila*) or devitellinated (*Danio*), hand sorted to isolate homozygous mutants where needed, and homogenized in TRizol (Invitrogen). RNA was then extracted as per manufacturer's specification. cDNA was generated using Superscript III (Invitrogen) and qPCR was performed with SYBR Green (Promega) using an ABI Prism 7000. Primers were designed to be intron spanning. qPCR reactions were run in triplicate and normalized to *RpL32* (*Drosophila*) or GAPDH (zebrafish) expression. Primer sequences are provided in supplementary material Table S6.

### Western blot

COS-1 cells were transfected with 1 μg of DNA according to manufacturer's instructions (Fugene6, Roche), maintained for 48 hours, collected and lysed with NP40 lysis buffer. Western blots were performed as described previously (Mokalled et al., 2010).

### Transgenes and site-directed mutagenesis

UAS constructs were generated by subcloning *hoip* (DGRC RE51843) and *NHP2L1* (DF/HCC HSCD00326196) ORFs into pUASt. HA-tagged Hoip was made by PCR amplifying the *hoip* ORF and cloning the PCR fragment into pEntr (Invitrogen); after sequence verification, L/R clonase (Invitrogen) was used to recombine *hoip* into THW. For reporter genes, genomic DNA was PCR amplified, cloned into pCRII (Invitrogen), sequence verified, subcloned into pH.Stinger.eGFP (Barolo et al., 2004). Transgenic vectors were injected by standard methods to establish stable transgenic insertions. Multiple independent lines were characterized for each construct. Primer sequences are available upon request. Site-directed mutagenesis to generate Hoip.-225GFP.ΔE was carried out as described previously (Johnson et al., 2011).

### RNA-Seq

The SOLiD Total RNA-Seq Kit was used for RNA purification from 6-10 hour embryos and DNA library construction. Libraries were prepared in duplicate and sequenced on a 5500xl SOLiD Sequencer (Life Technologies) using a paired-end reading strategy. Sequencing reads were mapped to the UCSC reference genome using LifeScope (Life Technologies), then assembled and quantified using the Cufflinks algorithm (Trapnell et al., 2010). Assembled sequence reads were visualized using the Integrative Genomics Viewer (Robinson et al., 2011) and GO analysis was performed using the DAVID 6.7 bioinformatics resources (Dennis et al., 2003).

### Zebrafish embryology

Fertilized, one-cell stage Tg(*α-actin:GFP*) zebrafish embryos were injected with 0.08 ng or 0.8 ng of *nhp2l1b* ATG-MO (GGTTCACTTCAGCTTCAGTCATCTT) or 0.8 ng of Cntrl-MO (Gene Tools). At 14 hpf, embryos were live imaged for GFP, fixed and analyzed for GFP and MF20 expression, or used for RNA isolation and qPCR analysis, by standard methods. Similar experiments were performed for *nhp2l1b* 5′UTR-MO (TTACTTAATAACACACGGTCCTCTC). Annealed oligonucleotides encoding the ATG-MO target sequence were cloned into 5′RV EGFP T7TS (Small et al., 2005). Linearized template was transcribed with T7 mMessage machine (Ambion) to generate injectable RNA. Control and morphant embryos were prepared and imaged in parallel.

## RESULTS

### A forward genetic screen identified hoip as an essential regulator of myogenesis

We performed an EMS genetic screen to identify novel mutations that specifically affect somatic muscle morphology. Our screening strategy employed two reporter genes: MHC.τGFP, which expresses a membrane-localized GFP in embryonic somatic muscles (Chen and Olson, 2001); and Hand.nGFP that expresses a nuclear-localized GFP in cardioblasts (CBs) by embryonic stage 12 (St12) (Johnson et al., 2011). The Hand.nGFP reporter served as a control to distinguish mutations that affected early mesoderm patterning events and cardiac cell fate specification, allowing us to focus on

mutations that specifically affected somatic muscle morphology. We screened ~10,000 genomes and identified 96 mutations on the second chromosome that caused somatic muscle defects (supplementary material Fig. S1A). We mapped two mutations to *Kon-tiki* (*Kon*), a known regulator of target site recognition (Schnorrer et al., 2007), and a second mutation to *mind bomb 2*, a known regulator of muscle attachment (Carrasco-Rando and Ruiz-Gómez, 2008).

One mutation that solely affected the pattern of MHC.τGFP expression mapped to a region of chromosome 2L that contains eight genes (Fig. 1A). Genetic analysis in this region showed that the mutation failed to complement *P{lacW}hoip*$^{k07104}$, so we named the EMS allele *hoip*$^{1}$. The Hoip orthologs Snu13 in yeast and NHP2L1 (Non-Histone Protein 2 Like-1) in humans are RNA-binding proteins that bind noncoding RNAs associated with the spliceosome (Dobbyn and O'Keefe, 2004; Vidovic et al., 2000; Watkins et al., 2002). Compared with live wild-type (WT) embryos (Fig. 1B), somatic muscle morphology was aberrant in live *hoip*$^{1}$ homozygous (Fig. 1C), *hoip*$^{1}$*/Df(2L)ED690* (Fig. 1D) and *hoip*$^{1}$*/P{lacW}hoip*$^{k07104}$ transheterozygous embryos (Fig. 1E). In particular, the lateral transverse (LT1-4), lateral longitudinal (LL1), lateral oblique (LO1) and dorsal oblique (DO3-5) somatic muscles showed pronounced membrane extensions towards target sites, yet remained rounded in *hoip* mutant embryos (Fig. 1C-E; supplementary material Table S1). This failure in myogenesis prevented *hoip*$^{1}$, *hoip*$^{1}$*/Df(2L)ED690* and *hoip*$^{1}$*/P{lacW}hoip*$^{k07104}$ embryos from emerging from the chorion after embryogenesis.

The *P{lacW}hoip*$^{k07104}$ insertion was originally identified in a peripheral nervous system (PNS) screen (Kania et al., 1995; Prokopenko et al., 2000). *P{lacW}hoip*$^{k07104}$ embryos showed

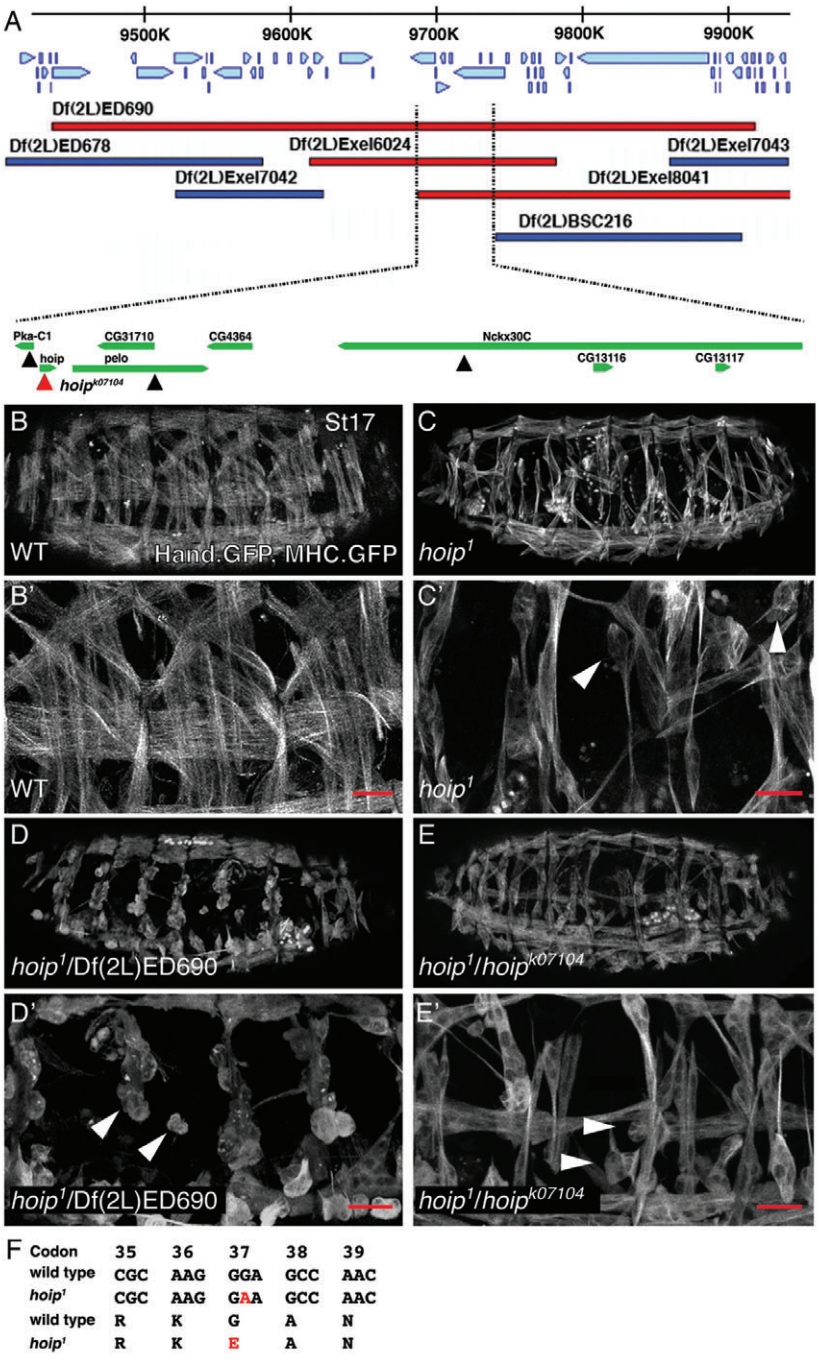


F

| Codon | 35 | 36 | 37 | 38 | 39 |
|---|---|---|---|---|---|
| wild type | CGC | AAG | GGA | GCC | AAC |
| *hoip*$^{1}$ | CGC | AAG | GAA | GCC | AAC |
| wild type | R | K | G | A | N |
| *hoip*$^{1}$ | R | K | E | A | N |

**Fig. 1. A mutation adversely affecting somatic muscle development maps to *hoip*.** (**A**) The genomic region uncovered by *Df(2L)ED690*. Genes and direction of transcription are shown with blue arrows. Deficiencies that fail to complement *hoip*$^{1}$ are shown in red; deficiencies that complement *hoip*$^{1}$ are shown in dark blue. The minimal overlapping area among the deficiencies that fail to complement *hoip*$^{1}$ contains eight genes. Of the four lethal transgene insertions (triangles) in the minimal overlapping area, only *P{lacW}hoip*$^{k07104}$ (red triangle) failed to complement *hoip*$^{1}$. (**B-E**) MHC.τGFP, Hand.nGFP expression in St17 embryos. (B) Wild-type embryos express membrane-localized τGFP in each somatic muscle in all embryonic segments. Somatic muscles are severely rounded (arrowheads) in *hoip*$^{1}$ (C), *hoip*$^{1}$*/Df(2L)ED690* (D) and *hoip*$^{1}$*/P{lacW}hoip*$^{k07104}$ embryos (E). (**B′-E′**) High-magnification views of embryos shown in B-E. (**F**) *hoip*$^{1}$ is a G37E missense mutation (see supplementary material Fig. S1I). In this and subsequent figures, embryos are oriented with anterior towards the left and dorsal towards the top. Coordinates refer to base pair positions on chromosome 2L. Scale bars: 20 μm.

disorganized dorsal clusters of PNS neurons and axonal path finding defects (Kania et al., 1995). However, the P-element itself was not revertible (Kania et al., 1995) and *P{lacW}hoip*$^{k07104}$ embryos showed global patterning defects that we did not observe in other *hoip* mutant combinations (supplementary material Fig. S1B,C). We assayed PNS morphology in *hoip*$^{1}$ and *hoip*$^{1}$/*P{lacW}hoip*$^{k07104}$ embryos ($n \geq 3$) but could not confirm the previously reported PNS defects (supplementary material Fig. S1D-F). These data suggest a lethal mutation on the *P{lacW}hoip*$^{k07104}$ chromosome outside *hoip* disrupts a powerful regulator of embryonic patterning that could affect PNS development.

Sequencing the *hoip*$^{1}$ allele revealed a G37E missense mutation (Fig. 1F; supplementary material Fig. S1I) within the predicted Hoip RNA-binding domain (Schultz et al., 2006). Based on the predicted crystal structure of this domain (supplementary material Fig. S1G), the acidic amino acid substitution would be expected to eliminate Hoip RNA-binding activity (Vidovic et al., 2000). A tagged *hoip* protein harboring the G37E mutation was detectable by western blot in transfected COS-1 cells, demonstrating that *hoip*$^{1}$ is not a protein null mutation (supplementary material Fig. S1H).

## Myotube elongation does not initiate in *hoip* embryos

To understand the stage of myogenesis regulated by Hoip, we performed time-lapse studies in embryos expressing τGFP under the control of the founder cell driver rp298.gal4. Our analysis focused on the LL, LT, LO and DO muscles, as these muscles were most often disrupted in *hoip* mutant embryos (supplementary material Table S1). Our analysis began in late St12 embryos that expressed rp298>τGFP in nascent myotubes (Fig. 2A). In wild-type embryos, myotubes showed obvious polarization and had elongated to 50% of segment width after 30 minutes. By 60 minutes, the myotubes had largely completed their extension and created extensive filopodia for attachment site recognition (Fig. 2A; $n$=2). By contrast, nascent myotubes failed to elongate in *hoip*$^{1}$ embryos after 30 minutes even though the myotubes showed an initial polarity (Fig. 2B). By 60 minutes, myotubes failed to extend to 50% of segment width in *hoip*$^{1}$ embryos and had lost their polarity (Fig. 2B; $n$=3). These results demonstrate that myotubes failed to elongate and reach their attachment sites in *hoip*$^{1}$ embryos.

To understand whether Hoip controls target site recognition, we repeated time-lapse imaging at higher magnification to document filopodia in detail (supplementary material Fig. S2; $n$=3). *hoip*$^{1}$ embryos extended filopodia exclusively in the direction of myotube polarity. This phenotype contrasts with that of *Kon* mutant embryos, which initiate myotube elongation but, instead of orienting filopodia solely toward muscle attachment sites, extend ectopic filopodia in all directions (Schnorrer et al., 2007). Kon is a transmembrane receptor that regulates myotube target site recognition. As *hoip* myotubes do not phenocopy *Kon* myotubes, we conclude that Hoip does not control attachment site recognition.

## Muscle attachment sites are specified in *hoip* embryos

To understand whether tendon cells, which mediate muscle attachment, were specified in *hoip*$^{1}$ embryos, we assayed expression of βPS (*myospheroid*), an effector of muscle attachment. βPS is expressed in tendon cells and localizes to myotendinous junctions after attachment-site recognition (Martin-Bermudo and Brown, 2000). βPS was clearly detectable in the epidermis of *hoip*$^{1}$ embryos, but showed diffuse localization along the dorsoventral axis compared with wild-type embryos (Fig. 2C,D). As βPS is also

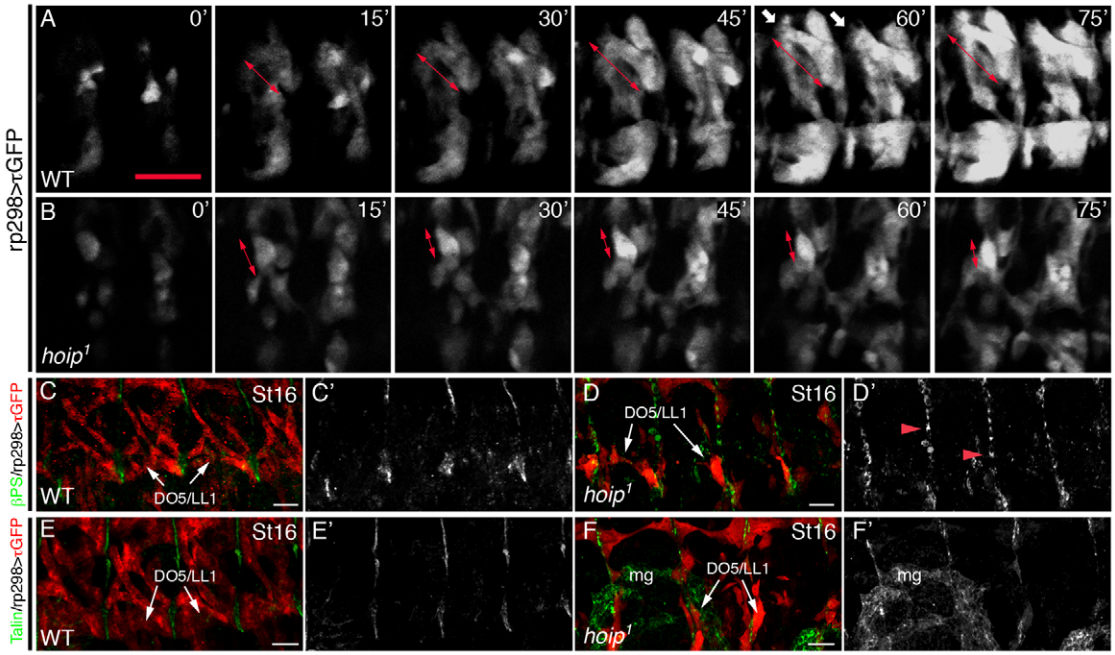


**Fig. 2. *hoip* embryos have myotube elongation defects.** (**A**,**B**) Time-lapse images of rp298>τGFP embryos initiated at late St12. (A) Wild-type embryos showed robust myotube elongation at 30 minutes (double arrows) and developed extensive filopodia for attachment site recognition at 60 minutes (white arrows). (B) Myotubes established polarity in *hoip*$^{1}$ embryos at 15 minutes but failed to elongate by 30 minutes. Polarized myofibers at 15 minutes compacted over time (double-headed arrows). (**C**,**D**) St16 rp298>τGFP embryos double labeled for GFP and βPS. (C) βPS localizes to myotendinous junctions in wild-type embryos. (D) Tendon cells express βPS in *hoip*$^{1}$ embryos but localization is diffuse (red arrowheads). (**C′**,**D′**) βPS expression alone. (**E**,**F**) St16 rp298>τGFP embryos double labeled for GFP and Talin. Talin is expressed in tendon cells of wild-type (E) and *hoip*$^{1}$ (F) embryos. (**E′**,**F′**) Talin expression alone. mg, midgut. Scale bars: 20 μm.

expressed in somatic muscle, we next examined Talin expression. Talin is restricted to tendon cells and acts as a linker between βPS and the cytoskeleton. Similar to βPS, Talin is clearly expressed in the epidermis of *hoip*$^{1}$ embryos (Fig. 2E,F). Taken together, these results show that the rounded muscle phenotype in *hoip*$^{1}$ embryos is due to a block at, or prior to, myotube elongation and is not a result of tendon cell mis-specification.

## Hoip does not regulate founder cell specification or the first round of myoblast fusion

To further characterize the myogenic phenotype in *hoip*$^{1}$ embryos, we examined founder cell specification and myoblast fusion. After specification, founder cells undergo an initial round of fusion that is complete by the end of St12 (Bate, 1990). Subsequent fusion then determines final muscle size and each muscle undergoes a unique number of fusion events. MHC serves as a classic marker for identifying myoblast fusion defects; embryos with defects in the first round of myoblast fusion robustly express MHC in single unfused founder cells (Chen and Olson, 2001). To control against possible dominant mutations on the EMS chromosome, we compared MHC expression in *hoip*$^{1}$ embryos with heterozygous *hoip*$^{1}$/Cyo.lacZ embryos. Strikingly, the somatic musculature of St16 *hoip*$^{1}$ embryos showed almost no MHC protein expression, whereas *hoip*$^{1}$/Cyo embryos showed normal MHC expression and somatic muscle morphology (Fig. 3A,B; Table 1).

Another method for identifying myoblast fusion defects is to quantify the temporal expression of muscle identity genes in the dorsal mesoderm (Chen and Olson, 2001). The identity gene *nautilus* (*nau*) is expressed in a subset of founder cells that give rise to the somatic muscles affected in *hoip*$^{1}$ embryos, including DA3, DO3, DO4, DO5, VA1, LO1 (Wei et al., 2007). The number of Nau+ nuclei in *hoip*$^{1}$ embryos was comparable with *hoip*$^{1}$/Cyo.lacZ embryos at St12, but significantly less at St14 (supplementary material Fig. S3A,B). Thus, founder cell specification and the first round of myoblast fusion proceed normally in *hoip*$^{1}$ embryos; however, the later rounds of fusion do not occur.

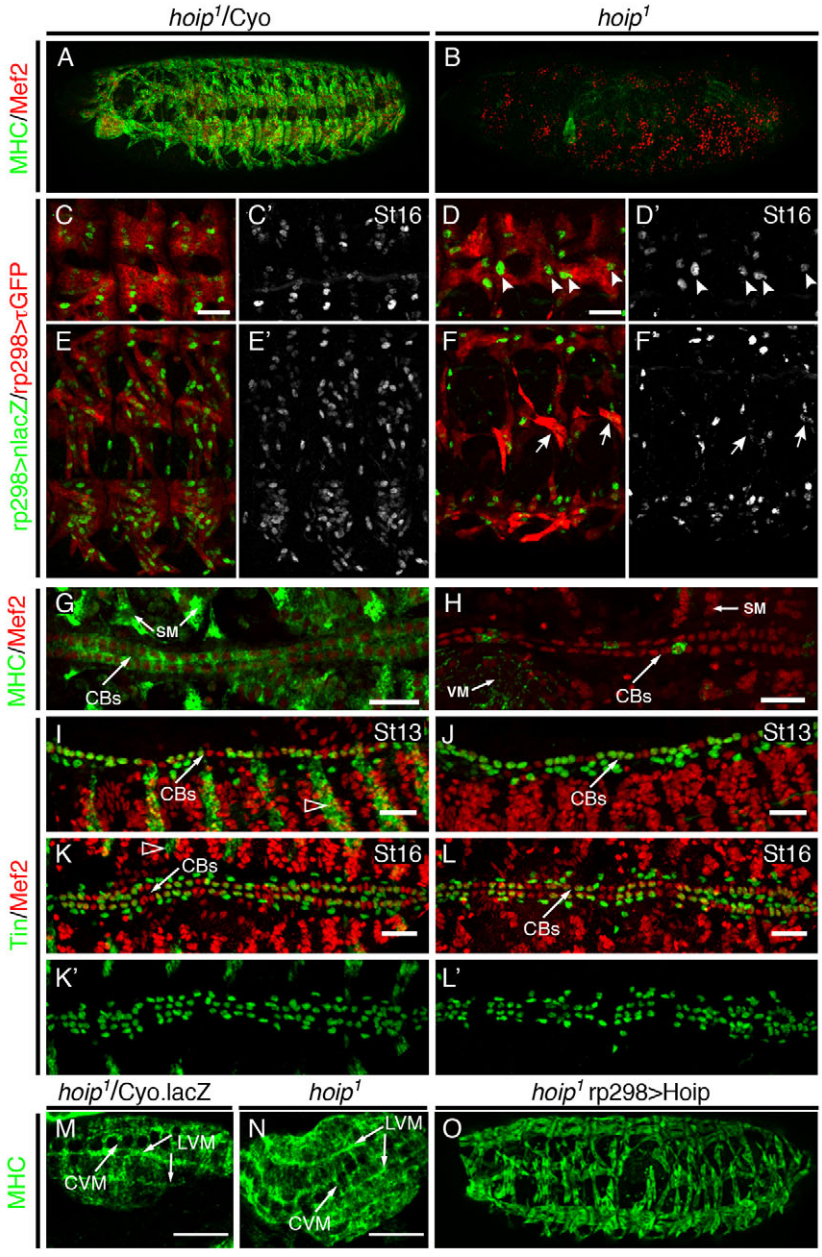


**Fig. 3. Hoip regulates somatic muscle and cardioblast maturation but not precursor specification.** (**A**,**B**) Mef2 and MHC protein expression in St16 embryos. Lateral views. Robust MHC and Mef2 expression is detectable in somatic muscles of *hoip*$^{1}$/Cyo.lacZ embryos (A). Mef2 expression is unaffected in *hoip*$^{1}$ embryos, whereas MHC is nearly absent from the somatic muscle (B). (C-F) St16 rp298.gal4>τ.GFP, rp298.nlacZ embryos double-labeled for GFP (red) and lacZ (green). (**C-D′**) Dorsal muscles. The number of lacZ$^{+}$ nuclei is reduced in *hoip*$^{1}$ embryos (C) compared with *hoip*$^{1}$/Cyo.lacZ embryos (D); however, binucleated dorsal muscles show complete elongation (arrowheads). (**E-F′**) Lateral and ventral muscles. The number of lacZ$^{+}$ nuclei is also reduced in lateral and ventral muscles in *hoip*$^{1}$ embryos. Multinucleate lateral muscles show incomplete elongation (arrows). (G,H) Mef2 and MHC protein expression in St16 embryos. Dorsal views. (**G**) *hoip*$^{1}$/Cyo.lacZ embryos express Mef2 and MHC in mature CBs. (**H**) *hoip*$^{1}$ embryos express Mef2 but not MHC in a great majority of CBs. (**I-L′**) Mef2 and Tin protein expression. (I,J) *hoip*$^{1}$/Cyo.lacZ embryos express Mef2 in all myogenic precursors, including CBs. Tin is expressed in four Mef2$^{+}$ CBs per hemisegment at St13 (I; lateral view) and St16 (K; dorsal view). Mef2 and Tin expression in *hoip*$^{1}$ CBs is comparable with control embryos at St13 (J) and St16 (L). (K′,L′) Tin expression alone. (**M**,**N**) High magnification micrographs of visceral muscles in St16 embryos. MHC expression is comparable between *hoip*$^{1}$/Cyo.lacZ embryos (M) and *hoip*$^{1}$ embryos (N). Both genotypes develop LVMs and CVMs in the visceral mesoderm. (**O**) *hoip*$^{1}$ rp298>Hoip embryos express MHC protein at near wild-type levels in the somatic mesoderm. SM, somatic muscle; VM, visceral muscle; LVM, longitudinal visceral muscle; CVM, circular visceral muscle; CBs, cardioblasts. Open arrowheads in I,K show ectodermal cytoplasmic *lacZ* expression that distinguishes *hoip*$^{1}$ heterozygotes from homozygotes. Scale bars: 20 μm.

**Table 1. MHC expression**

| Genotype | *hoip*$^{1}$/Cyo | *hoip*$^{1}$ | *hoip*$^{1}$ Rp298 >Hoip | *hoip*$^{1}$ Rp298 >NHP2L1 |
|---|---|---|---|---|
| MHC+ myofibers* | 10.31±1.16 | 1.40±1.12 | 7.48±1.56 | 6.00±1.82 |
| *n* | 26 | 35 | 24 | 21 |
| #LT1-LT4 | 130/136 | 3/136 | 52/128 | 35/88 |

*Twelve lateral muscles assayed including DO3-5, DA3, DT1, LT1-4, LL1-LO1 and SBM.

To confirm this result, we used the founder cell transgene rp298.nlacZ to assay founder cell specification and myoblast fusion. Similar to Nau, the number of *lacZ*-positive nuclei was comparable between *hoip*$^{1}$ and *hoip*$^{1}$/Cyo.lacZ embryos at St12 (supplementary material Fig. S3C,D), but significantly reduced at St14 and St16 (Fig. 3C-F; supplementary material Fig. S3E-H). However, the fusion defects in *hoip*$^{1}$ embryos were not restricted to the muscles that showed elongation defects. For example, DO1 and DA1 muscles elongated normally in *hoip*$^{1}$ embryos but showed dramatically fewer lacZ-positive nuclei than *hoip*$^{1}$/Cyo.lacZ embryos (Fig. 3C,D). However, LL1 and LO5 were multinucleate in *hoip*$^{1}$ embryos but failed to elongate (Fig. 3E,F).

## Somatic and cardiac muscle maturation is Hoip dependent

One explanation for the somatic muscle defects in *hoip*$^{1}$ embryos was that MHC itself is required for myotube elongation. However, embryos homozygous for the null mutation *MHC*$^{1}$ (Wells et al., 1996) showed normal myotube elongation (supplementary material Fig. S3I,J). Sarcomere assembly occurs after myotube elongation and myofiber attachment (Rui et al., 2010) and embryos defective for the first round of myoblast fusion do express MHC (Chen and Olson, 2001). Together, these observations demonstrate that muscle morphogenesis is genetically separable from muscle structural expression and prompted us to define a secondary role for Hoip during myogenesis.

In *Drosophila*, MHC is the single muscle myosin and is expressed in cardiac, somatic and visceral muscle (Bernstein et al., 1983). Mef2 is also expressed in all myogenic cells and is a direct transcriptional activator of MHC (Bour et al., 1995). Mef2 was expressed at comparable levels in the somatic and cardiac mesoderm of *hoip*$^{1}$ and *hoip*$^{1}$/Cyo.lacZ embryos (Fig. 3A,B,G-L), even though MHC was largely absent from both tissues in *hoip*$^{1}$ embryos (Fig. 3B,H). The expression of a second transcription factor, Tinman (Tin), is restricted to and orchestrates the maturation of a subset of cardioblasts (CBs) (Reim et al., 2005). Cardiac Tin expression was also comparable between *hoip*$^{1}$ and *hoip*$^{1}$/Cyo.lacZ embryos (Fig. 3I-L). As *Drosophila* CBs are mononucleate, do not undergo elongation, yet fail to express MHC in *hoip*$^{1}$ embryos, we conclude that Hoip regulates muscle maturation (i.e. muscle structural protein expression) independently of myotube elongation.

Even though MHC expression was largely absent from CBs and somatic muscles in *hoip*$^{1}$ embryos, MHC expression in mature visceral muscle was comparable between *hoip*$^{1}$ and *hoip*$^{1}$/Cyo.lacZ embryos (Fig. 3M,N). These results suggest that Hoip performs tissue-specific functions during myogenesis to specifically regulate striated muscle maturation.

## Hoip regulates terminal muscle differentiation

To confirm that Hoip regulates myogenesis after founder cell specification, we expressed Hoip with rp298.Gal4 in *hoip*$^{1}$ embryos and assayed MHC expression. Founder cell-specific expression of Hoip was indeed sufficient to rescue myotube elongation and MHC protein expression in somatic muscles of *hoip*$^{1}$ embryos (Fig. 3O; Table 1). Hoip therefore regulates myogenesis after founder cell specification in a mesoderm cell-autonomous manner.

## *hoip* is expressed in striated but not visceral muscle progenitors

*In situ* hybridization using a probe antisense to the full-length *hoip* transcript (Fig. 4A) showed *hoip* expression initiates at low levels in the mesoderm and endoderm of St9 embryos (supplementary material Fig. S4A-C). Robust expression *hoip* mRNA could be detected in St11 embryos and, consistent with the tissue-restricted MHC phenotype in *hoip*$^{1}$ embryos, is expressed in the Mef2-expressing cells of the somatic and cardiac mesoderm, but not in the Mef2-expressing cells of the visceral mesoderm (Fig. 4B). *hoip* mRNA is also expressed in the fat body and the endoderm at this stage, but is absent from the neuroectoderm ventral to the Mef2 expression domain. *hoip* mRNA continues to be expressed in the somatic musculature throughout embryogenesis (Fig. 4C; supplementary material Fig. S4D,E). We did not detect *hoip* in the PNS by *in situ* hybridization.

To confirm the *in situ* results, we generated a GFP reporter construct that contained 225 bp of genomic DNA upstream of the *hoip*-coding sequence (Hoip.-225.GFP). This reporter gene directed GFP expression in a pattern that recapitulated *hoip* mRNA expression in St11 and St13 embryos (Fig. 4D,E). Interestingly, the Hoip.-225 sequence contains a conserved E-box sequence (CANNTG, supplementary material Fig. S4F). Basic helix-loop-helix (bHLH) transcription factors bind E-box sequences and a *hoip* reporter gene with a mutated E-box (Hoip.-225ΔE.GFP) initiated GFP expression in a manner comparable with Hoip.-225.GFP (Fig. 4F) but did not maintain GFP expression in the mesoderm through St13 (Fig. 4G). These findings demonstrate that *hoip* is expressed in the striated muscle lineage after precursor cell specification, and that maintenance of *hoip* expression depends on a conserved E-box sequence that is likely a bHLH target.

We next assayed Hoip localization in the somatic musculature using an HA-tagged Hoip transgene. Surprisingly, Mef2>Hoip-HA embryos showed both nuclear and cytoplasmic localization of Hoip-HA (supplementary material Fig. S5). Hoip may thus perform multiple molecular functions during myogenesis.

## Several sarcomeric genes are downregulated in *hoip* embryos

The Hoip orthologs Snu13 in yeast and NHP2L1 in humans are spliceosomal RNA-binding proteins (Dobbyn and O'Keefe, 2004; Vidovic et al., 2000; Watkins et al., 2002). In eukaryotes, spliceosomes that contain small nuclear (sn) RNAs are believed to remove intronic sequences from pre-mRNAs, whereas spliceosomes that contain small nucleolar (sno) RNAs orchestrate ordered cleavages along pre-rRNAs. Snu13/NHP2L1 proteins preferentially bind to GA-rich RNA sequences in the kink-turn motif of both snRNAs and snoRNAs (Cléry et al., 2007; Nottrott et al., 1999; Schultz et al., 2006; Vidovic et al., 2000).

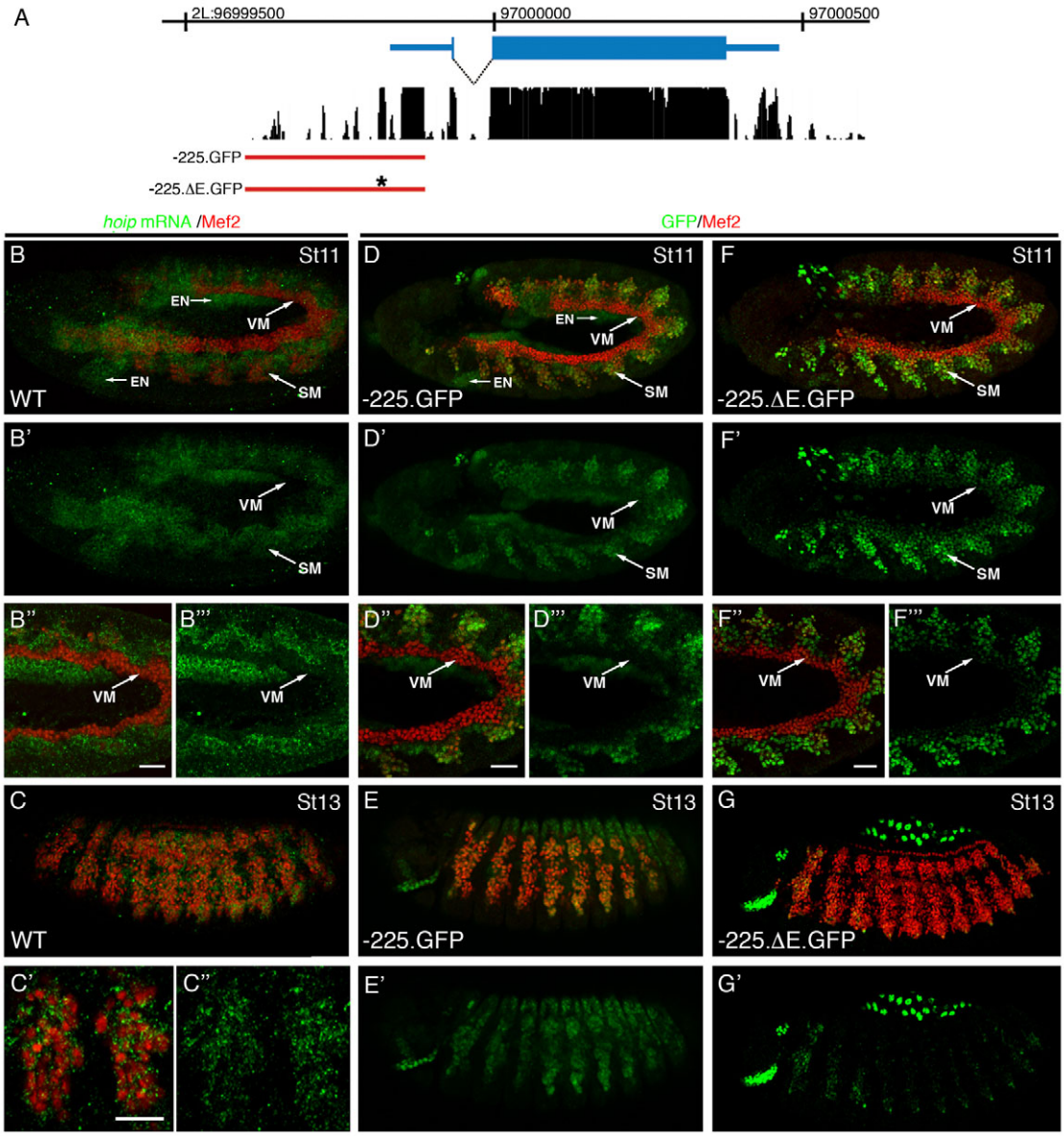


**Fig. 4. *hoip* is expressed in striated but not visceral muscle progenitors.** (**A**) *hoip* gene organization and conservation within the *Drosophila* genus. The red line identifies genomic sequences used to generate the −225.nGFP and −225ΔE.nGFP *hoip* reporter genes. (**B**) St11 embryo labeled for *hoip* mRNA (green) and Mef2 (red). *hoip* mRNA is expressed in the Mef2-expressing cells of the somatic mesoderm, as well as in the fat body and the endoderm, but is absent from the neuroectoderm. (**B′**) *hoip* expression alone. (**B″**,**B‴**) High magnification micrograph of the mesoderm shows *hoip* mRNA expression in the somatic but not the visceral mesoderm. (**C-C″**) At St13, *hoip* mRNA is still detectable in the developing somatic musculature. (**D-E′**) Hoip.-225.GFP embryos labeled for GFP (green) and Mef2 (red). GFP expression recapitulates hoip mRNA expression at St11 (D) and St13 (E). (**F-G′**) Hoip.-225ΔE.GFP embryos labeled for GFP (green) and Mef2 (red). GFP expression recapitulates *hoip* mRNA expression at St11 (F) but is undetectable at St13 (G). SM, somatic mesoderm; VM, visceral mesoderm; EN, endoderm. Scale bars: 20 μm.

We took a non-biased approach to identify potential Hoip targets in the developing mesoderm. As robust *hoip* expression initiates at St11 and continues at high levels through St13, we performed RNA-seq in St11-13 (6-10 hour) embryos. Our analysis identified 353 transcripts that were differentially expressed and 60 transcripts that were expressed approximately at wild-type levels but inappropriately processed in $hoip^{1}$ embryos (supplementary material Tables S2, S3). This RNA-seq analysis also identified the G37E missense mutation in $hoip^{1}$ embryos, confirming the initial genomic sequencing data. In addition, 45S pre-rRNA was processed correctly in $hoip^{1}$ St11-13 embryos, suggesting that Hoip does not regulate ribosome biogenesis during these stages of development (supplementary material Fig. S6A). These *in vivo* results demonstrate that Hoip is not required to process all pre-mRNA or pre-rRNA transcripts during embryogenesis.

We analyzed the misregulated transcripts in $hoip^{1}$ embryos by Gene Ontology (GO) functional annotation clustering and found the most significant cluster associated with the GO term Contractile Fiber (Fig. 5A). Strikingly, transcripts within the Contractile Fiber cluster (Table 2) include *Mhc* and other sarcomere components, including *inflated* (*if*), *Myosin light chain 2* (*Mlc2*), *Tropomyosin 2* (*Tm2*), *Troponin C at 47D* (*TpnC47D*) and *Troponin C at 73F* (*TpnC73F*). We confirmed the RNA-seq data for these sarcomeric

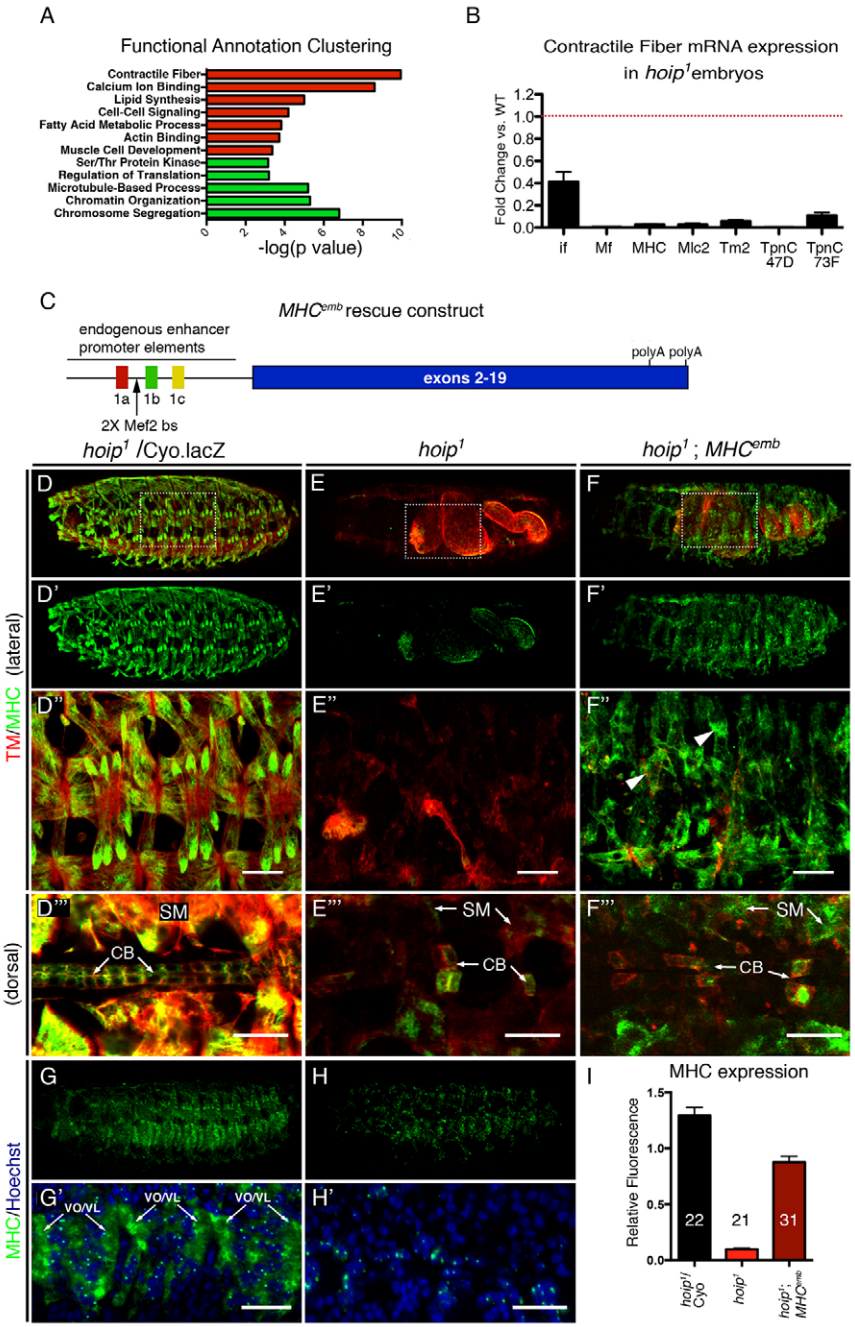


**Fig. 5. Hoip processes transcripts encoding sarcomere components.** (**A**) Functional Gene Ontology (GO) analysis of misregulated transcripts in *hoip*$^{1}$ embryos. Clusters of down- and upregulated transcripts are shown in red and green, respectively. The most significant cluster is associated with the term Contractile Fiber. (**B**) qPCR of Contractile Fiber transcript expression in *hoip*$^{1}$ embryos compared with wild type. (**C**) The *MHC*$^{emb}$ transgene. The construct contains endogenous, somatic muscle *MHC* enhancer elements, multiple transcriptional start sites (colored 1st exons), an embryonic *MHC* cDNA and the endogenous poly A sites. bs, binding site. (**D-F‴**) St16 embryos double-labeled for Tropomyosin (Tm) and MHC. Compared with *hoip*$^{1}$/Cyo.lacZ embryos (D), both MHC and Tm are largely undetectable in the somatic and cardiac musculature of *hoip*$^{1}$ embryos (E). In *hoip*$^{1}$*; MHC*$^{emb}$ embryos, MHC protein expression is restored to near wild-type levels in somatic but not cardiac muscles; Tm remains largely undetectable in *hoip*$^{1}$*; MHC*$^{emb}$ embryos (F). *MHC*$^{emb}$ does not rescue somatic muscle morphology defects (arrowheads) or MHC expression in cardioblasts (CBs). The Tm antibody recognizes both Tm1 and Tm2: RNA-seq showed a 0.50 (Tm1) and 0.09 (Tm2) fold change in *hoip*$^{1}$ embryos compared with wild type (Table 2). (G,H) St16 embryos co-labeled for MHC mRNA and Hoechst. (**G**,**G′**) MHC mRNA shows both nuclear and cytoplasmic localization in the somatic muscle fibers of control embryos. (**H**,**H′**) MHC mRNA is exclusively detected in somatic muscle nuclei of *hoip*$^{1}$ embryos. High magnification views in G′ and H′ show three segments of ventral oblique (VO) and ventral lateral (VL) muscles. (**I**) Quantification of MHC expression in the somatic musculature. Mean fluorescent intensity was calculated for lateral muscles over an entire segment (see supplementary material Fig. S7). The number of segments assayed is given for each genotype. Error bars represent s.e.m. Scale bars: 20 μm.

genes by quantitative PCR (qPCR) and found that each transcript was dramatically downregulated in *hoip*$^{1}$ embryos compared with controls (Fig. 5B). The RNA-seq data showed that the embryonic sarcomeric actins *Act57B* and *Act87E*, and *Mef2*, the only known robust transcriptional regulator of terminal muscle differentiation genes in *Drosophila*, were expressed at wild-type levels in *hoip*$^{1}$ embryos (supplementary material Fig. S6B, Table S2). The developmental time point of our RNA-seq coincided with the onset of muscle structural gene expression at St12. However, *hoip*$^{1}$ embryos fail to express MHC protein at all developmental stages (Fig. 3B). These observations suggest that Hoip is required to both initiate and maintain muscle structural gene expression during embryogenesis.

We examined 22 genes experimentally shown to regulate myotube elongation, attachment site recognition or myotendinous junction formation in our RNA-seq data (supplementary material Table S4). Surprisingly, *pav* expression was not changed in *hoip*$^{1}$ embryos, whereas *tum* was upregulated (fold change=2.04). However, *tum* overexpression does not affect myotube elongation (Guerin and Kramer, 2009b). Of the remaining 19 genes, only *MSP-300* showed significant downregulation in *hoip*$^{1}$ embryos (fold change=0.27). Unlike *hoip*$^{1}$ embryos, *MSP-300* mutant embryos show only a modest somatic muscle phenotype that initiates late in embryogenesis (Rosenberg-Hasson et al., 1996); however, *MSP-300* larvae do show defects in nuclear positioning and microtubule organization (Elhanany-Tamir et al., 2012). The 22 genes regulating somatic muscle morphology also showed normal splicing in *hoip*$^{1}$ embryos, further arguing that Hoip regulates the expression of other transcripts to initiate myotube elongation.

**Table 2. Contractile fiber mRNA expression**

| Gene | Molecular function | Fold change* |
|---|---|---|
| *bent* | Sarcomere organization | 0.055 |
| *inflated* | Adhesion molecule binding | 0.558 |
| *Myofilin* | Unknown | 0.010 |
| *Myosin alkali light chain 1* | ATPase activity | 0.067 |
| *Myosin heavy chain* | Actin binding | 0.054 |
| *Myosin light chain 2* | ATPase activity | 0.093 |
| *Tropomyosin 1* | Actin binding | 0.500 |
| *Tropomyosin 2* | Actin binding | 0.010 |
| *Troponin C at 47D* | Calcium ion binding | 0.038 |
| *Troponin C at 73F* | Calcium ion binding | 0.016 |
| *upheld (Troponin T)* | Calcium ion binding | 0.074 |
| *wings up A* | Tropomyosin binding | 0.071 |
| *Zasp66* | Protein phosphatase binding | 0.013 |

*Fold change in 6-10 hour *hoip*$^{1}$ embryos assayed by RNA-seq.

## Post-transcriptional regulation of MHC

The RNA analyses suggested that Hoip processes pre-mRNAs encoding sarcomeric proteins but does not regulate transcription or rRNA processing. To confirm these results, we performed a functional rescue experiment with the *MHC*$^{emb}$ transgene (Fig. 5C), which uses the endogenous *MHC* promoter to express a *MHC* cDNA specifically in somatic muscle (Hess et al., 2007; Wells et al., 1996). If Hoip regulated either ribosome biogenesis or processing of an mRNA whose protein product activates *MHC* transcription, then *MHC*$^{emb}$ would not be expected to rescue MHC protein expression in *hoip*$^{1}$ embryos. However, if Hoip acts post-transcriptionally to splice the *MHC* pre-mRNA, then the *MHC* cDNA, which is expressed from the *MHC*$^{emb}$ transgene, would generate a functional mRNA that would be appropriately translated in *hoip*$^{1}$ embryos.

Indeed, the *MHC*$^{emb}$ transgene restored MHC protein expression in somatic but not cardiac muscle of *hoip*$^{1}$ embryos (Fig. 5D-F,I; supplementary material Fig. S7). This experiment corroborated our MHC.τGFP expression studies in which the endogenous MHC promoter directed GFP protein expression throughout the somatic mesoderm of *hoip*$^{1}$ embryos (Fig. 1C-E). In addition, the *MHC*$^{emb}$ transgene did not restore somatic muscle morphology in *hoip*$^{1}$ embryos, further confirming that Hoip regulates myotube elongation independent of MHC expression. We conclude Hoip is required to perform at least one splice in the *MHC* pre-mRNA and functions independently of ribosome biogenesis to direct somatic muscle maturation.

## MHC mRNA does not translocate out of the nucleus in *hoip* embryos

Two separate transgenes harboring MHC promoters (MHC.τGFP and MHC$^{emb}$) were able to direct cDNA expression in *hoip*$^{1}$ embryos (Fig. 1C, Fig. 5F). However, *MHC* mRNA was nearly undetectable in *hoip*$^{1}$ embryos by RNA-seq and qPCR (Fig. 5B). We assayed *MHC* mRNA localization by *in situ* hybridization and found only punctate, nuclear *MHC* mRNA localization in *hoip*$^{1}$ embryos, even though wild-type embryos showed *MHC* mRNA localized throughout the myofiber (Fig. 5G,H). These transgenic and *in situ* results clearly demonstrate that *MHC* is transcribed in *hoip*$^{1}$ embryos but that the transcript fails to translocate out of the nucleus.

## Hoip orthologs are essential regulators of myogenesis

The remarkable homology between Hoip and human NHP2L1 (supplementary material Fig. S1I) suggested that the function of

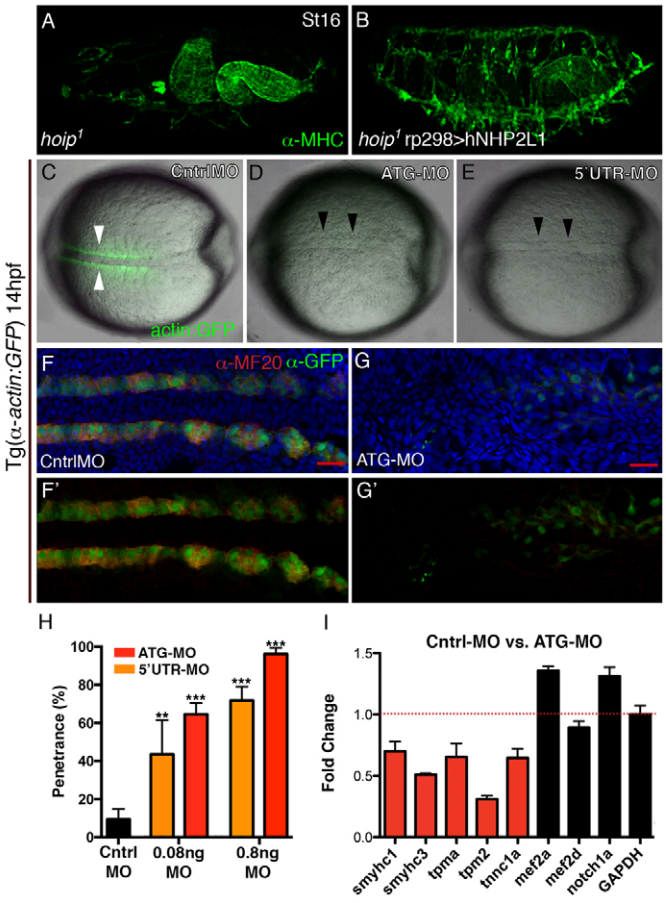


**Fig. 6. Hoip is a conserved regulator of myogenesis.** (**A**,**B**) St16 *Drosophila* embryos labeled for MHC protein. Compared with *hoip*$^{1}$ embryos (A), *hoip*$^{1}$ rp298>human NHP2L1 embryos show a significant restoration of MHC protein expression and muscle morphology in the somatic mesoderm (B). (**C-E**) Dorsal views of 14 hpf Tg (*α-actin:GFP*) zebrafish embryos. Embryos injected with control MO at the one-cell stage express robust GFP in somites (C, white arrowheads). Embryos injected with *nhp2l1b* ATG-MO (D) or 5′UTR-MO (E) do not initiate GFP expression. ATG-MO and 5′UTR-MO embryos develop a distinguishable neural tube by 14 hpf (black arrowheads). (**F-G′**) Dorsal view of 14 hpf Tg(*α-actin:GFP*) zebrafish embryos labeled for GFP and MF20 (which reacts with muscle MyHC isoforms). Embryos injected with control MO show robust GFP and MF20 expression in the somatic mesoderm (F), whereas ATG-MO injected embryos display little or no GFP or MF20 staining (G). (**H**) Dose-dependent response to *nhp2l1b* MOs. Percent penetrance was calculated as the number of embryos without detectable GFP fluorescence, relative to all injected embryos. Significance between ATG-MO/5′UTR-MO and Cntrl MO was calculated using a *t*-test. ***P*<0.01, ****P*<0.001. (**I**) qPCR of mesoderm transcript expression. Relative expression was calculated as mRNA levels in control versus ATG-MO-injected embryos after normalization to GAPDH. Error bars represent s.e.m.

Hoip during myogenesis is conserved across species. To test this hypothesis, we expressed human NHP2L1 in founder cells of *hoip*$^{1}$ embryos with rp298.gal4 and assayed MHC protein expression. Although human NHP2L1 did not rescue *hoip*$^{1}$ embryos as effectively as *Drosophila* Hoip (Table 1), we observed a significant restoration of myotube elongation and MHC expression in the somatic musculature, demonstrating that Hoip and human NHP2L1 can perform similar functions during myogenesis (Fig. 6A,B).

Zebrafish *nhp2l1b* is expressed in the paraxial mesoderm at 10 hour post-fertilization (hpf) and throughout the myotome at 19 hpf

(Thisse and Thisse, 2001). We asked whether *nhp2l1b* is essential for zebrafish muscle development using two independent MOs to knockdown endogenous *nhp2l1b*. One MO targets the *nhp2l1b* translational start site with 100% identity (ATG-MO), but does not target the highly divergent *nhp2l1a* (supplementary material Fig. S8A-C). The other MO targets the *nhp2l1b* 5′UTR 57 bp upstream of the translational start site and shows no sequence similarity to *nhp2l1a* (supplementary material Fig. S8B). The *α-actin:GFP* transgenic (Tg) line harbors a skeletal muscle reporter (Higashijima et al., 1997) and Tg(*α-actin:GFP*) embryos injected with control-MO showed robust GFP expression in the somitic mesoderm by 14 hpf (Fig. 6C). However, both ATG-MO- and 5′UTR-MO-injected embryos showed little or no GFP expression (Fig. 6D,E). The MF20 antibody reacts with all muscle MyHC isoforms, and we observed robust somitic MF20 staining in control-MO but not ATG-MO-injected embryos at 14 hpf (Fig. 6F,G).

Tg(*α-actin:GFP*) expression showed a dose-dependent response to MO concentrations (Fig. 6H). Sixty-five percent ($n$=259) of embryos injected with 0.08 ng ATG-MO and 96% ($n$=233) of embryos injected with 0.8 ng ATG-MO failed to initiate α-actin:GFP expression; 43% ($n$=58) of embryos injected with 0.08 ng 5′UTR-MO and 72% ($n$=87) of embryos injected with 0.8 ng 5′UTR-MO failed to initiate α-actin:GFP expression; 11% ($n$=302) of embryos injected with 0.8 ng Cntrl-MO showed changes in α-actin:GFP expression. With the exception of skeletal muscle marker expression, 0.8 ng ATG-MO-treated embryos appeared normal through 16 hpf; however, MO treatment induced lethality after 16 hpf (supplementary material Fig. S8F,G). The ATG-MO also blocked eGFP translation when the *nhp2l1b* ATG-MO target site was placed upstream of the eGFP-coding sequence (supplementary material Fig. S8D,E). Thus, the ATG-MO targets *nhp2l1b*.

By qPCR, we found that several transcripts encoding sarcomeric proteins were present at reduced levels in ATG-MO 14 hpf embryos, including two slow MyHCs, two troponins and one tropomyosin. Importantly, the expression of other genes essential for mesoderm development, such as *mef2* and *notch1*, was unaffected in ATG-MO embryos. Taken together, these results indicate that the function of Hoip is highly conserved and that *nhp2l1b* regulates myogenesis in vertebrates.

## DISCUSSION

The results of this study reveal a specific and essential role for the putative RBP Hoip in the control of embryonic muscle development. *hoip* is expressed in the striated muscle lineage and regulates two distinct processes: myotube elongation and sarcomeric protein expression. Using functional rescue experiments, we have established that Hoip regulates *MHC* pre-mRNA splicing but not *MHC* transcription. The human *hoip* ortholog human *NHP2L1* can rescue myogenesis in *hoip* mutant embryos, and antisense *nhp2l1b* knockdown blocks muscle development in zebrafish. This study is the first to identify a tissue-specific function for *hoip* or its orthologs *in vivo* and highlights the essential role of post-transcriptional gene regulation during tissue morphogenesis.

Non-coding RNAs that function as ‘core’ spliceosome components can have tissue-specific functions *in vivo*. For example, the mouse genome encodes multiple U2 snRNA genes and the *rnu2-8* U2 snRNA is differentially expressed in the mouse nervous system with peak expression levels in the cerebellum (Jia et al., 2012). *Rnu2-8* knockout mice show normal splicing of constitutive exons, but incomplete splicing of alternative exons solely within the cerebellum (Jia et al., 2012), and *rnu2-8* U2 snRNA is essential for neuron survival in the cerebellum.

The Hoip orthologs Snu13/NHP2L1 proteins have been characterized as ‘core’ spliceosome components that bind the kink turn motif of U4 snRNAs, U3 snoRNAs and U14 snoRNAs (Schultz et al., 2006). However, we found Hoip expression and function is restricted to the striated muscle lineage within the *Drosophila* mesoderm. RNA-seq and $MHC^{emb}$ rescue data clearly demonstrate that Hoip is not a global regulator of pre-mRNA splicing or ribosome biogenesis, but acts specifically on a set of RNAs that encode functionally related proteins.

The $MHC^{emb}$ transgene contains a fully spliced *MHC* cDNA that encodes exons 2-19 (Wells et al., 1996). The 5′ end of the transgene comprises genomic DNA that initiates 450 bp upstream of the first transcriptional start site and terminates in exon 2. This 5′ sequence contains the necessary enhancer and promoter elements for transgene expression in the somatic mesoderm, as well as three alternative transcriptional start sites. The 3′ end of the transgene contains a complete exon 19 with multiple polyadenylation (poly A) sites, but it does not contain an exogenous poly A signal (i.e. SV40). As $MHC^{emb}$ rescues MHC protein expression in *hoip* embryos, Hoip must not regulate transcriptional start site selection or 5′UTR stability. In addition, the endogenous 3′UTR is sufficient to restore MHC protein expression, indicating that Hoip does not regulate poly A site choice, polyadenylation itself or 3′UTR stability. Hoip therefore acts post-transcriptionally to control at least one splicing event in exons 2-19.

The apparent specificity with which Hoip targets sarcomeric RNAs is striking. One explanation for this specificity is that the Hoip paralog Nhp2 fulfills the spliceosome functions that Hoip does not. A more intriguing hypothesis is that Hoip facilitates ribonucleotide modifications in a subset of transcripts. For example, NHP2L1/snoRNA processomes direct 2′-O methylation of ribosomal pre-RNAs (Watkins et al., 2002) and 2′-O methylation has been reported to enhance pre-mRNA splicing in some contexts (Ge et al., 2010). Perhaps Hoip confers a similar modification to sarcomeric RNAs that is permissive for pre-mRNA splicing; in this model, unmodified pre-mRNAs would not be spliced and would degrade in the nucleus. We envision Hoip-mediated modifications to be a rate-limiting step that ensures proper stoichiometry of sarcomeric proteins.

This study also identified myotube elongation defects in *hoip* embryos. To our knowledge, this is the first mutation reported that blocks the initiation of myotube elongation (supplementary material Table S4). Accordingly, we failed to identify robust misregulation of genes known to regulate myotube elongation, attachment site recognition or myotendinous junction formation in *hoip* embryos (supplementary material Table S4). The strength of the *hoip* phenotype suggests that a suite of proteins is required for myotube elongation. A second possibility is that some sarcomeric proteins could be required for myotube elongation. We have shown that *MHC* does not regulate elongation; however, tropomyosins regulate actin dynamics outside the sarcomere that influence cell polarity and cell outgrowth in *Drosophila* (Li and Gao, 2003; Zimyanin et al., 2008).

One known regulator of microtubule dynamics during elongation, Tum, is a Rac family GTPase-activating protein (RacGAP). We searched the RNA-seq data for other Rac/Rho family regulators and identified two RhoGAPs and one Rho guanine nucleotide exchange factor (RhoGEF) that were misregulated in *hoip* embryos (supplementary material Table S5). We also identified two Rab family GTPases, the function of which in synaptic endosome trafficking has been well established (Gurkan et al., 2005). Rab family members are essential for microtubule-dependent outgrowth

of tracheal and bristle cells (Nagaraj and Adler, 2012; Schottenfeld-Roames and Ghabrial, 2012) and the myotube guidance molecule Grip localizes to endosomes at the ends of extending myotubes (Swan et al., 2004). Finally, overexpressing the tendon cell regulator Stripe in the ectoderm upregulates a number of novel genes (Gilsohn and Volk, 2010a; Gilsohn and Volk, 2010b), including the transmembrane protein Tetraspanin 42Ea (Tsp42Ea). Tsp42Ea orthologs function in cell motility and signal transduction, and *Tsp42Ea* was downregulated in *hoip* embryos. It will be interesting to determine which of these genes are required for myotube elongation *in vivo*.

The zebrafish Hoip ortholog *nhp2l1b* is expressed in the paraxial mesoderm during the 10- to 14-somite stage and in the myotome during the 20- to 25-somite stage (Thisse and Thisse, 2001). Thus, the expression and myogenic function of *hoip*/*nhp2l1b* appears to be conserved in vertebrates. Despite being one of the most intensely studied developmental systems, skeletal muscle continues to reveal novel developmental mechanisms. In the future, it will be of particular interest to characterize the interactions between transcriptional and post-transcriptional mechanisms that coordinate final muscle morphology and function.

**Acknowledgements**
We appreciate Mike Buszczak for insights and discussions throughout this study. We thank Sandy Bernstein, Elizabeth Chen, Richard Cripps and Bruce Paterson for reagents.

**Funding**
E.N.O. is supported by grants from the National Institutes of Health (NIH) [HL-077439], The American Heart Association (AHA)-Jon Holden DeHaan Foundation [0970518N], Foundation Leducq Networks of Excellence, Cancer Prevention & Research Institute of Texas and the Robert A. Welch Foundation [1-0025]. A.N.J. is supported by a Scientist Development Grant [12SDG12030160] from the AHA. K.D.P. is supported by the NIH [GM074057 and HL081674]. Deposited in PMC for release after 12 months.

**Competing interests statement**
The authors declare no competing financial interests.

**Author contributions**
Experiments were carried out by A.N.J., M.H.M. and J.M.V. Experimental design, analyses and preparation of the manuscript were carried out by A.N.J., M.H.M., J.M.V., K.D.P. and E.N.O.

**Supplementary material**
Supplementary material available online at
http://dev.biologists.org/lookup/suppl/doi:10.1242/dev.095596/-/DC1

**References**

**Barolo, S., Castro, B. and Posakony, J. W.** (2004). New Drosophila transgenic reporters: insulated P-element vectors expressing fast-maturing RFP. *Biotechniques* **36**, 436-440, 442.
**Bate, M.** (1990). The embryonic development of larval muscles in Drosophila. *Development* **110**, 791-804.
**Bernstein, S. I., Mogami, K., Donady, J. J. and Emerson, C. P., Jr** (1983). Drosophila muscle myosin heavy chain encoded by a single gene in a cluster of muscle mutations. *Nature* **302**, 393-397.
**Biedermann, B., Hotz, H. R. and Ciosk, R.** (2010). The Quaking family of RNA-binding proteins: coordinators of the cell cycle and differentiation. *Cell Cycle* **9**, 1929-1933.
**Bloor, J. W. and Brown, N. H.** (1998). Genetic analysis of the Drosophila alphaPS2 integrin subunit reveals discrete adhesive, morphogenetic and sarcomeric functions. *Genetics* **148**, 1127-1142.
**Bour, B. A., O'Brien, M. A., Lockwood, W. L., Goldstein, E. S., Bodmer, R., Taghert, P. H., Abmayr, S. M. and Nguyen, H. T.** (1995). Drosophila MEF2, a transcription factor that is essential for myogenesis. *Genes Dev.* **9**, 730-741.
**Brown, N. H.** (1994). Null mutations in the alpha PS2 and beta PS integrin subunit genes have distinct phenotypes. *Development* **120**, 1221-1231.
**Brown, N. H., Gregory, S. L., Rickoll, W. L., Fessler, L. I., Prout, M., White, R. A. and Fristrom, J. W.** (2002). Talin is essential for integrin function in Drosophila. *Dev. Cell* **3**, 569-579.
**Bunch, T. A., Graner, M. W., Fessler, L. I., Fessler, J. H., Schneider, K. D., Kerschen, A., Choy, L. P., Burgess, B. W. and Brower, D. L.** (1998). The PS2 integrin ligand tiggrin is required for proper muscle function in Drosophila. *Development* **125**, 1679-1689.
**Callahan, C. A., Bonkovsky, J. L., Scully, A. L. and Thomas, J. B.** (1996). derailed is required for muscle attachment site selection in Drosophila. *Development* **122**, 2761-2767.
**Carmena, A., Bate, M. and Jiménez, F.** (1995). Lethal of scute, a proneural gene, participates in the specification of muscle progenitors during Drosophila embryogenesis. *Genes Dev.* **9**, 2373-2383.
**Carrasco-Rando, M. and Ruiz-Gómez, M.** (2008). Mind bomb 2, a founder myoblast-specific protein, regulates myoblast fusion and muscle stability. *Development* **135**, 849-857.
**Chanana, B., Graf, R., Koledachkina, T., Pflanz, R. and Vorbrüggen, G.** (2007). AlphaPS2 integrin-mediated muscle attachment in Drosophila requires the ECM protein Thrombospondin. *Mech. Dev.* **124**, 463-475.
**Chen, E. H. and Olson, E. N.** (2001). Antisocial, an intracellular adaptor protein, is required for myoblast fusion in Drosophila. *Dev. Cell* **1**, 705-715.
**Cléry, A., Senty-Ségault, V., Leclerc, F., Raué, H. A. and Branlant, C.** (2007). Analysis of sequence and structural features that identify the B/C motif of U3 small nucleolar RNA as the recognition site for the Snu13p-Rrp9p protein pair. *Mol. Cell. Biol.* **27**, 1191-1206.
**de Joussineau, C., Bataillé, L., Jagla, T. and Jagla, K.** (2012). Diversification of muscle types in Drosophila: upstream and downstream of identity genes. *Curr. Top. Dev. Biol.* **98**, 277-301.
**Dennis, G., Jr, Sherman, B. T., Hosack, D. A., Yang, J., Gao, W., Lane, H. C. and Lempicki, R. A.** (2003). DAVID: Database for annotation, visualization, and integrated discovery. *Genome Biol.* **4**, 3.
**Dobbyn, H. C. and O'Keefe, R. T.** (2004). Analysis of Snu13p mutations reveals differential interactions with the U4 snRNA and U3 snoRNA. *RNA* **10**, 308-320.
**Elhanany-Tamir, H., Yu, Y. V., Shnayder, M., Jain, A., Welte, M. and Volk, T.** (2012). Organelle positioning in muscles requires cooperation between two KASH proteins and microtubules. *J. Cell Biol.* **198**, 833-846.
**Estrada, B., Gisselbrecht, S. S. and Michelson, A. M.** (2007). The transmembrane protein Perdido interacts with Grip and integrins to mediate myotube projection and attachment in the Drosophila embryo. *Development* **134**, 4469-4478.
**Folker, E. S., Schulman, V. K. and Baylies, M. K.** (2012). Muscle length and myonuclear position are independently regulated by distinct Dynein pathways. *Development* **139**, 3827-3837.
**Frommer, G., Vorbrüggen, G., Pasca, G., Jäckle, H. and Volk, T.** (1996). Epidermal egr-like zinc finger protein of Drosophila participates in myotube guidance. *EMBO J.* **15**, 1642-1649.
**Ge, J., Liu, H. and Yu, Y. T.** (2010). Regulation of pre-mRNA splicing in Xenopus oocytes by targeted 2′-O-methylation. *RNA* **16**, 1078-1085.
**Gilsohn, E. and Volk, T.** (2010a). Slowdown promotes muscle integrity by modulating integrin-mediated adhesion at the myotendinous junction. *Development* **137**, 785-794.
**Gilsohn, E. and Volk, T.** (2010b). A screen for tendon-specific genes uncovers new and old components involved in muscle-tendon interaction. *Fly (Austin)* **4**, 149-153.
**Guerin, C. M. and Kramer, S. G.** (2009a). Cytoskeletal remodeling during myotube assembly and guidance: coordinating the actin and microtubule networks. *Commun. Integr. Biol.* **2**, 452-457.
**Guerin, C. M. and Kramer, S. G.** (2009b). RacGAP50C directs perinuclear gamma-tubulin localization to organize the uniform microtubule array required for Drosophila myotube extension. *Development* **136**, 1411-1421.
**Gurkan, C., Lapp, H., Alory, C., Su, A. I., Hogenesch, J. B. and Balch, W. E.** (2005). Large-scale profiling of Rab GTPase trafficking networks: the membrome. *Mol. Biol. Cell* **16**, 3847-3864.
**Hess, N. K., Singer, P. A., Trinh, K., Nikkhoy, M. and Bernstein, S. I.** (2007). Transcriptional regulation of the Drosophila melanogaster muscle myosin heavy-chain gene. *Gene Expr. Patterns* **7**, 413-422.
**Higashijima, S., Okamoto, H., Ueno, N., Hotta, Y. and Eguchi, G.** (1997). High-frequency generation of transgenic zebrafish which reliably express GFP in whole muscles or the whole body by using promoters of zebrafish origin. *Dev. Biol.* **192**, 289-299.
**Jagla, T., Bellard, F., Lutz, Y., Dretzen, G., Bellard, M. and Jagla, K.** (1998). ladybird determines cell fate decisions during diversification of Drosophila somatic muscles. *Development* **125**, 3699-3708.
**Jia, Y., Mu, J. C. and Ackerman, S. L.** (2012). Mutation of a U2 snRNA gene causes global disruption of alternative splicing and neurodegeneration. *Cell* **148**, 296-308.
**Johnson, A. N., Burnett, L. A., Sellin, J., Paululat, A. and Newfeld, S. J.** (2007). Defective decapentaplegic signaling results in heart overgrowth and reduced cardiac output in Drosophila. *Genetics* **176**, 1609-1624.
**Johnson, A. N., Mokalled, M. H., Haden, T. N. and Olson, E. N.** (2011). JAK/Stat signaling regulates heart precursor diversification in Drosophila. *Development* **138**, 4627-4638.

**Kania, A., Salzberg, A., Bhat, M., D'Evelyn, D., He, Y., Kiss, I. and Bellen, H. J.** (1995). P-element mutations affecting embryonic peripheral nervous system development in Drosophila melanogaster. *Genetics* **139**, 1663-1678.
**Kiehart, D. P. and Feghali, R.** (1986). Cytoplasmic myosin from Drosophila melanogaster. *J. Cell Biol.* **103**, 1517-1525.
**Kosman, D., Small, S. and Reinitz, J.** (1998). Rapid preparation of a panel of polyclonal antibodies to Drosophila segmentation proteins. *Dev. Genes Evol.* **208**, 290-294.
**Kramer, S. G., Kidd, T., Simpson, J. H. and Goodman, C. S.** (2001). Switching repulsion to attraction: changing responses to slit during transition in mesoderm migration. *Science* **292**, 737-740.
**Kronert, W. A., O'Donnell, P. T. and Bernstein, S. I.** (1994). A charge change in an evolutionarily-conserved region of the myosin globular head prevents myosin and thick filament accumulation in Drosophila. *J. Mol. Biol.* **236**, 697-702.
**Li, W. and Gao, F. B.** (2003). Actin filament-stabilizing protein tropomyosin regulates the size of dendritic fields. *J. Neurosci.* **23**, 6171-6175.
**Lilly, B., Zhao, B., Ranganayakulu, G., Paterson, B. M., Schulz, R. A. and Olson, E. N.** (1995). Requirement of MADS domain transcription factor D-MEF2 for muscle formation in Drosophila. *Science* **267**, 688-693.
**Martin-Bermudo, M. D. and Brown, N. H.** (2000). The localized assembly of extracellular matrix integrin ligands requires cell-cell contact. *J. Cell Sci.* **113**, 3715-3723.
**Mokalled, M. H., Johnson, A., Kim, Y., Oh, J. and Olson, E. N.** (2010). Myocardin-related transcription factors regulate the Cdk5/Pctaire1 kinase cascade to control neurite outgrowth, neuronal migration and brain development. *Development* **137**, 2365-2374.
**Nagaraj, R. and Adler, P. N.** (2012). Dusky-like functions as a Rab11 effector for the deposition of cuticle during Drosophila bristle development. *Development* **139**, 906-916.
**Nose, A., Isshiki, T. and Takeichi, M.** (1998). Regional specification of muscle progenitors in Drosophila: the role of the msh homeobox gene. *Development* **125**, 215-223.
**Nottrott, S., Hartmuth, K., Fabrizio, P., Urlaub, H., Vidovic, I., Ficner, R. and Lührmann, R.** (1999). Functional interaction of a novel 15.5kD [U4/U6.U5] tri-snRNP protein with the 5′ stem-loop of U4 snRNA. *EMBO J.* **18**, 6119-6133.
**Prokopenko, S. N., He, Y., Lu, Y. and Bellen, H. J.** (2000). Mutations affecting the development of the peripheral nervous system in Drosophila: a molecular screen for novel proteins. *Genetics* **156**, 1691-1715.
**Reim, I., Mohler, J. P. and Frasch, M.** (2005). Tbx20-related genes, mid and H15, are required for tinman expression, proper patterning, and normal differentiation of cardioblasts in Drosophila. *Mech. Dev.* **122**, 1056-1069.
**Robinson, J. T., Thorvaldsdóttir, H., Winckler, W., Guttman, M., Lander, E. S., Getz, G. and Mesirov, J. P.** (2011). Integrative genomics viewer. *Nat. Biotechnol.* **29**, 24-26.
**Rosenberg-Hasson, Y., Renert-Pasca, M. and Volk, T.** (1996). A Drosophila dystrophin-related protein, MSP-300, is required for embryonic muscle morphogenesis. *Mech. Dev.* **60**, 83-94.
**Rui, Y., Bai, J. and Perrimon, N.** (2010). Sarcomere formation occurs by the assembly of multiple latent protein complexes. *PLoS Genet.* **6**, e1001208.
**Schejter, E. D. and Baylies, M. K.** (2010). Born to run: creating the muscle fiber. *Curr. Opin. Cell Biol.* **22**, 566-574.
**Schnorrer, F. and Dickson, B. J.** (2004). Muscle building; mechanisms of myotube guidance and attachment site selection. *Dev. Cell* **7**, 9-20.
**Schnorrer, F., Kalchhauser, I. and Dickson, B. J.** (2007). The transmembrane protein Kon-tiki couples to Dgrip to mediate myotube targeting in Drosophila. *Dev. Cell* **12**, 751-766.
**Schottenfeld-Roames, J. and Ghabrial, A. S.** (2012). Whacked and Rab35 polarize dynein-motor-complex-dependent seamless tube growth. *Nat. Cell Biol.* **14**, 386-393.
**Schultz, A., Nottrott, S., Watkins, N. J. and Lührmann, R.** (2006). Protein-protein and protein-RNA contacts both contribute to the 15.5K-mediated assembly of the U4/U6 snRNP and the box C/D snoRNPs. *Mol. Cell. Biol.* **26**, 5146-5154.
**Small, E. M., Warkman, A. S., Wang, D. Z., Sutherland, L. B., Olson, E. N. and Krieg, P. A.** (2005). Myocardin is sufficient and necessary for cardiac gene expression in Xenopus. *Development* **132**, 987-997.
**Steigemann, P., Molitor, A., Fellert, S., Jäckle, H. and Vorbrüggen, G.** (2004). Heparan sulfate proteoglycan syndecan promotes axonal and myotube guidance by slit/robo signaling. *Curr. Biol.* **14**, 225-230.
**Subramanian, A., Wayburn, B., Bunch, T. and Volk, T.** (2007). Thrombospondin-mediated adhesion is essential for the formation of the myotendinous junction in Drosophila. *Development* **134**, 1269-1278.
**Swan, L. E., Wichmann, C., Prange, U., Schmid, A., Schmidt, M., Schwarz, T., Ponimaskin, E., Madeo, F., Vorbrüggen, G. and Sigrist, S. J.** (2004). A glutamate receptor-interacting protein homolog organizes muscle guidance in Drosophila. *Genes Dev.* **18**, 223-237.
**Swan, L. E., Schmidt, M., Schwarz, T., Ponimaskin, E., Prange, U., Boeckers, T., Thomas, U. and Sigrist, S. J.** (2006). Complex interaction of Drosophila GRIP PDZ domains and Echinoid during muscle morphogenesis. *EMBO J.* **25**, 3640-3651.
**Thisse, B. and Thisse, C.** (2001). *Fast Release Clones: A High Throughput Expression Analysis*. ZFIN Direct Data Submission. http://zfin.org
**Toledano-Katchalski, H., Nir, R., Volohonsky, G. and Volk, T.** (2007). Post-transcriptional repression of the Drosophila midkine and pleiotrophin homolog miple by HOW is essential for correct mesoderm spreading. *Development* **134**, 3473-3481.
**Trapnell, C., Williams, B. A., Pertea, G., Mortazavi, A., Kwan, G., van Baren, M. J., Salzberg, S. L., Wold, B. J. and Pachter, L.** (2010). Transcript assembly and quantification by RNA-Seq reveals unannotated transcripts and isoform switching during cell differentiation. *Nat. Biotechnol.* **28**, 511-515.
**Venkatesh, T. V., Park, M., Ocorr, K., Nemaceck, J., Golden, K., Wemple, M. and Bodmer, R.** (2000). Cardiac enhancer activity of the homeobox gene tinman depends on CREB consensus binding sites in Drosophila. *Genesis* **26**, 55-66.
**Vidovic, I., Nottrott, S., Hartmuth, K., Lührmann, R. and Ficner, R.** (2000). Crystal structure of the spliceosomal 15.5kD protein bound to a U4 snRNA fragment. *Mol. Cell* **6**, 1331-1342.
**Watkins, N. J., Dickmanns, A. and Lührmann, R.** (2002). Conserved stem II of the box C/D motif is essential for nucleolar localization and is required, along with the 15.5K protein, for the hierarchical assembly of the box C/D snoRNP. *Mol. Cell. Biol.* **22**, 8342-8352.
**Wayburn, B. and Volk, T.** (2009). LRT, a tendon-specific leucine-rich repeat protein, promotes muscle-tendon targeting through its interaction with Robo. *Development* **136**, 3607-3615.
**Wei, Q., Rong, Y. and Paterson, B. M.** (2007). Stereotypic founder cell patterning and embryonic muscle formation in Drosophila require nautilus (MyoD) gene function. *Proc. Natl. Acad. Sci. USA* **104**, 5461-5466.
**Wells, L., Edwards, K. A. and Bernstein, S. I.** (1996). Myosin heavy chain isoforms regulate muscle function but not myofibril assembly. *EMBO J.* **15**, 4454-4459.
**Yarnitzky, T., Min, L. and Volk, T.** (1998). An interplay between two EGF-receptor ligands, Vein and Spitz, is required for the formation of a subset of muscle precursors in Drosophila. *Mech. Dev.* **79**, 73-82.
**Zhai, R. G., Hiesinger, P. R., Koh, T. W., Verstreken, P., Schulze, K. L., Cao, Y., Jafar-Nejad, H., Norga, K. K., Pan, H., Bayat, V. et al.** (2003). Mapping Drosophila mutations with molecularly defined P element insertions. *Proc. Natl. Acad. Sci. USA* **100**, 10860-10865.
**Zhang, S. and Bernstein, S. I.** (2001). Spatially and temporally regulated expression of myosin heavy chain alternative exons during Drosophila embryogenesis. *Mech. Dev.* **101**, 35-45.
**Zimyanin, V. L., Belaya, K., Pecreaux, J., Gilchrist, M. J., Clark, A., Davis, I. and St Johnston, D.** (2008). In vivo imaging of oskar mRNA transport reveals the mechanism of posterior localization. *Cell* **134**, 843-853.

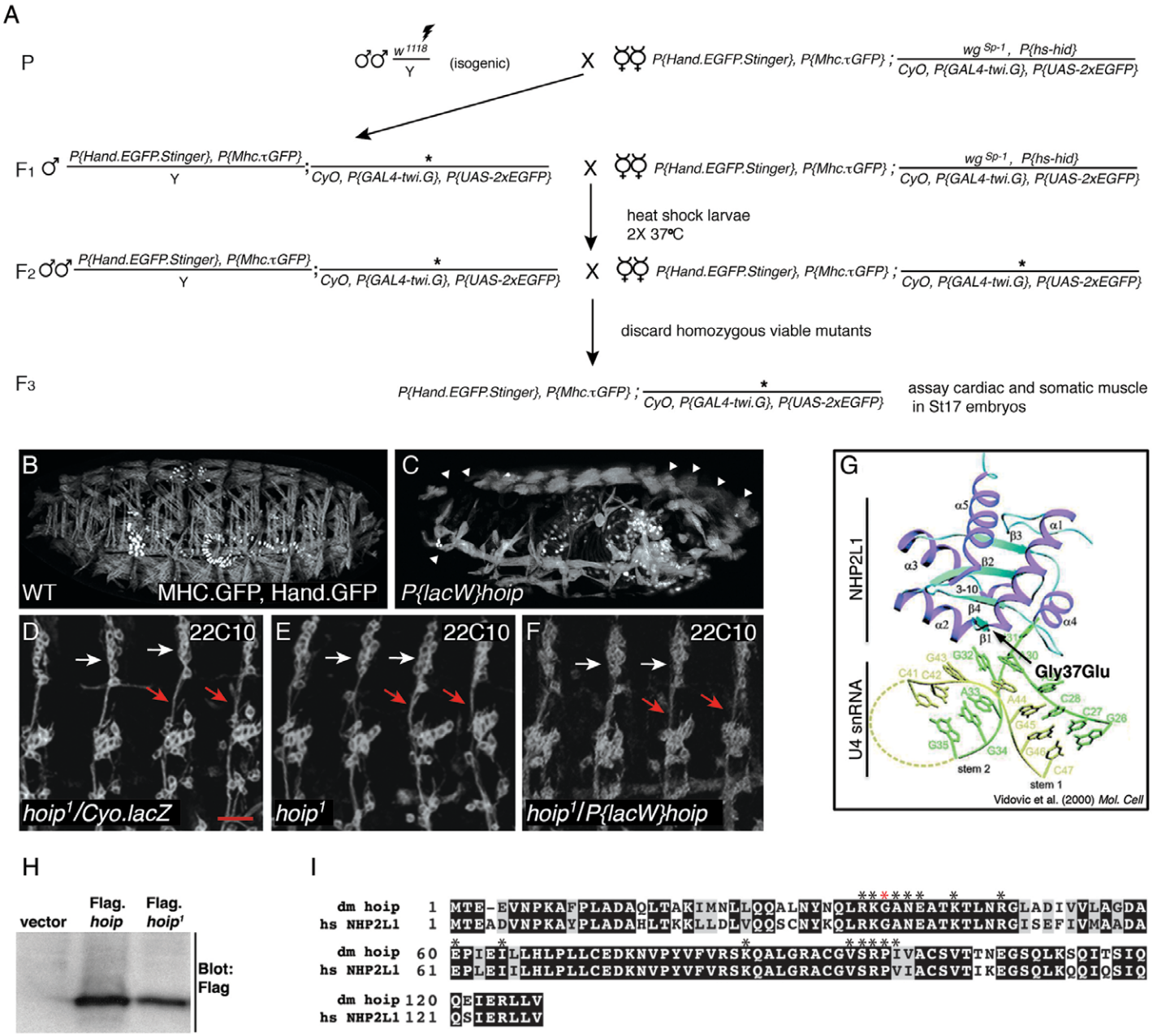


**Fig. S1. A forward genetic screen identified Hoip as a novel regulator of mesoderm development.** (**A**) Crossing scheme to generate EMS mutants in a double GFP reporter background. Over 10,000 mutagenized genomes were screened. (**B**,**C**) MHC.τGFP, Hand.n-GFP expression in St17 embryos. Compared with wild-type embryos (B), *P{lacW}hoip*$^{k07104}$ homozygous embryos (C) show severe muscle defects and apparent segmentation defects (white arrowheads). (**D-F**) St16 embryos stained with the PNS marker 22C10. Micrographs show four dorsal neuron clusters. The organization of the dorsal clusters (white arrows) and the pathway of the descending nerve (red arrows) are comparable among *hoip*$^{1}$*/Cyo* (D), *hoip*$^{1}$ (E) and *hoip*$^{1}$*/P{lacW}hoip*$^{k07104}$ (F) embryos. (**G**) Crystal structure of hNHP2L1 bound to U4 snRNA as reported previously (Vidovic et al., 2000), except the position of the 37th residue (mutated in *hoip*$^{1}$ embryos) is shown. (**H**) α-Flag western blot from COS cells transfected with empty pcDNA.Flag, pcDNA.Flag.Hoip or pcDNA.Flag.Hoip$^{1}$. (**I**) Alignment of Hoip and hNHP2L1 protein sequence. The two proteins are 79% identical and 89% similar. hNHP2L1 amino acids required for RNA binding are indicated with an asterisk (Schultz et al., 2006). The red asterisk shows the position of the *hoip*$^{1}$ missense mutation. Scale bar: 20μm.

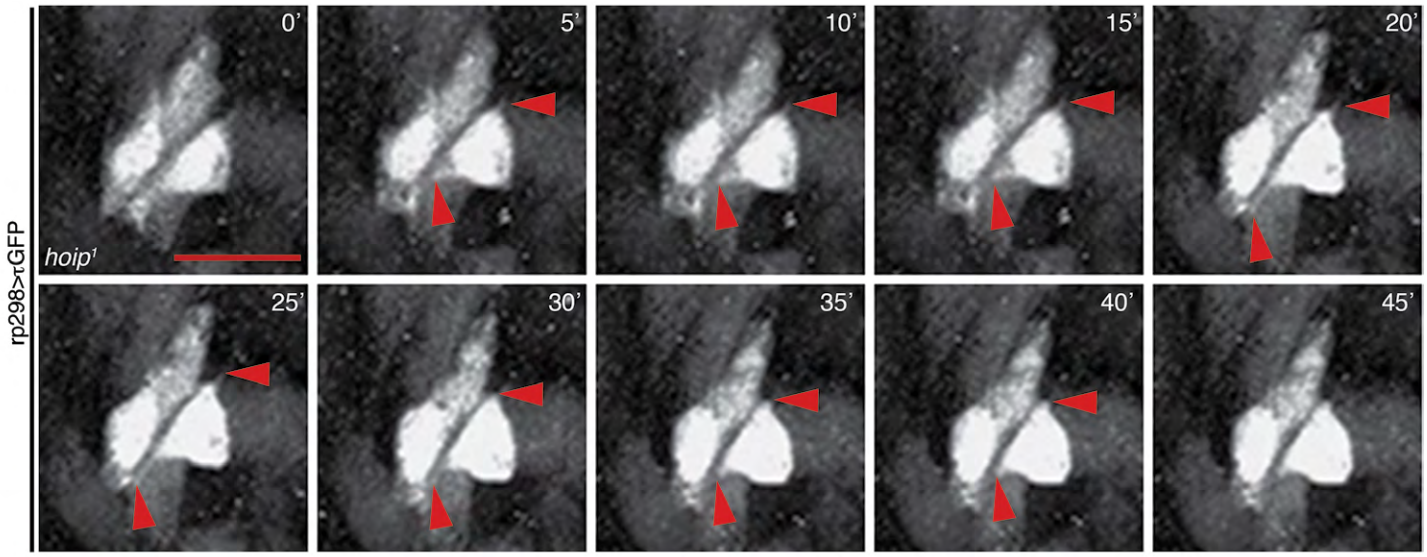


**Fig. S2. Somatic muscles in *hoip* embryos extend filapodia in the direction of polarization.** Time-lapse images of rp298. gal4>τGFP *hoip*$^{1}$ somatic muscles beginning at late St12. Filapodia extend in the axis of myotube polarization (red arrowheads) and then retract. Scale bar: 10 μm.

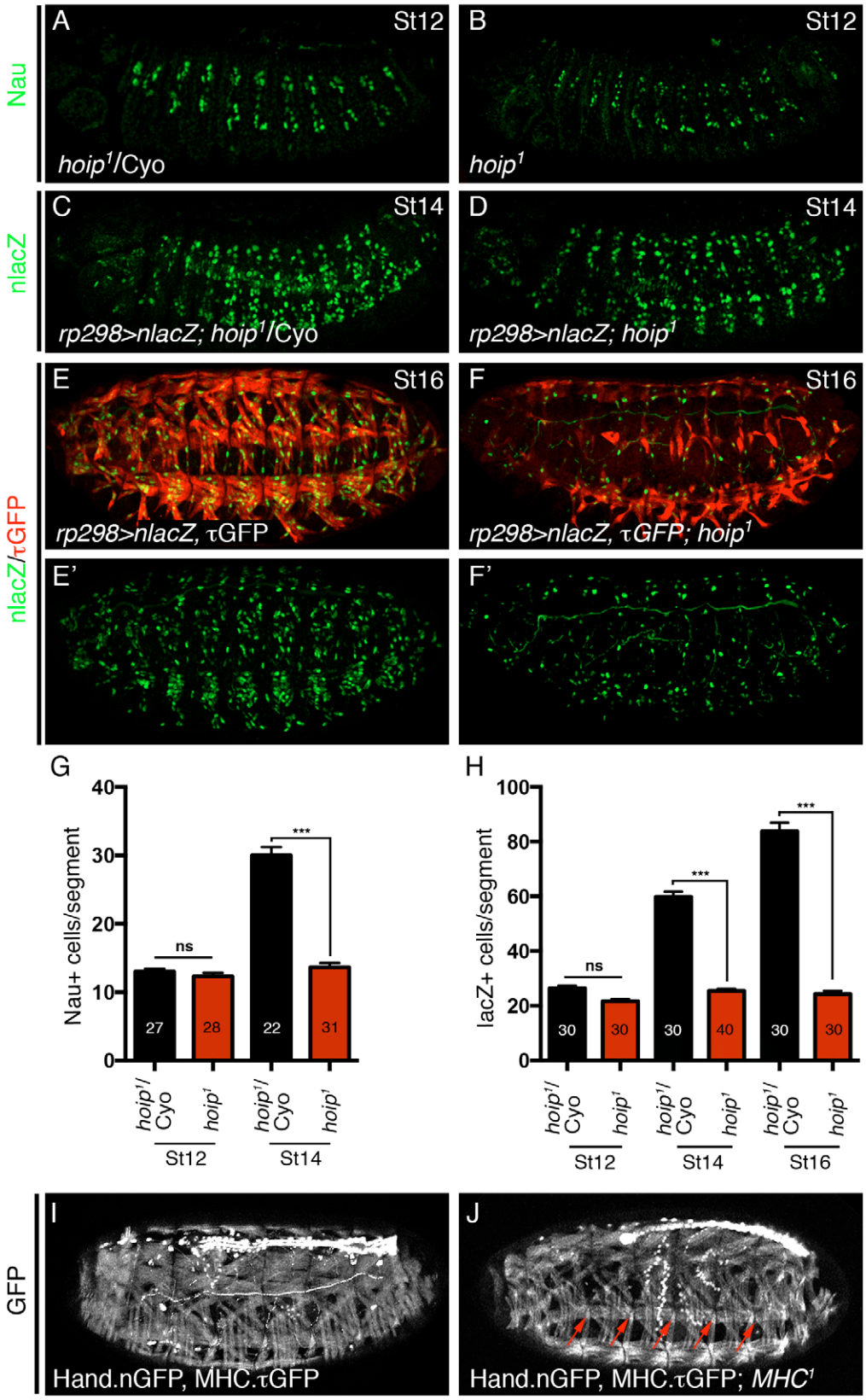


**Fig. S3. Muscle morphology and identity gene expression.** (**A**,**B**) Nau expression in St12 embryos. The number of Nau+ nuclei is comparable between control and *hoip*$^{1}$ embryos. (**C**,**D**) rp298.lacZ expression in St12 embryos. The number of lacZ$^{+}$ nuclei is comparable between control and *hoip*$^{1}$ embryos. (**E**,**F**) St16 rp298.gal4>τ.GFP, rp298.nlacZ embryos double-labeled for GFP (red) and lacZ (green). *hoip*$^{1}$ embryos showed a significant reduction in the number of lacZ$^{+}$ nuclei (F) compared with wild type (E). (**G**,**H**) Quantification of Nau$^{+}$ and rp298.lacZ$^{+}$ positive nuclei in the dorsal mesoderm. The number of segments quantified is given for each genotype and time point. Unpaired *t*-tests were performed to establish significance. Error bars represent s.e.m. (**I**,**J**) MHC.τGFP, Hand.nGFP expression in St16 embryos. (I) Wild-type and (J) *MHC*$^{1}$ embryos show similar somatic muscle morphology. In particular LL1/DO5 muscles have elongated and attached in all segments (red arrows). ns, not significant; ***$P$<0.001.

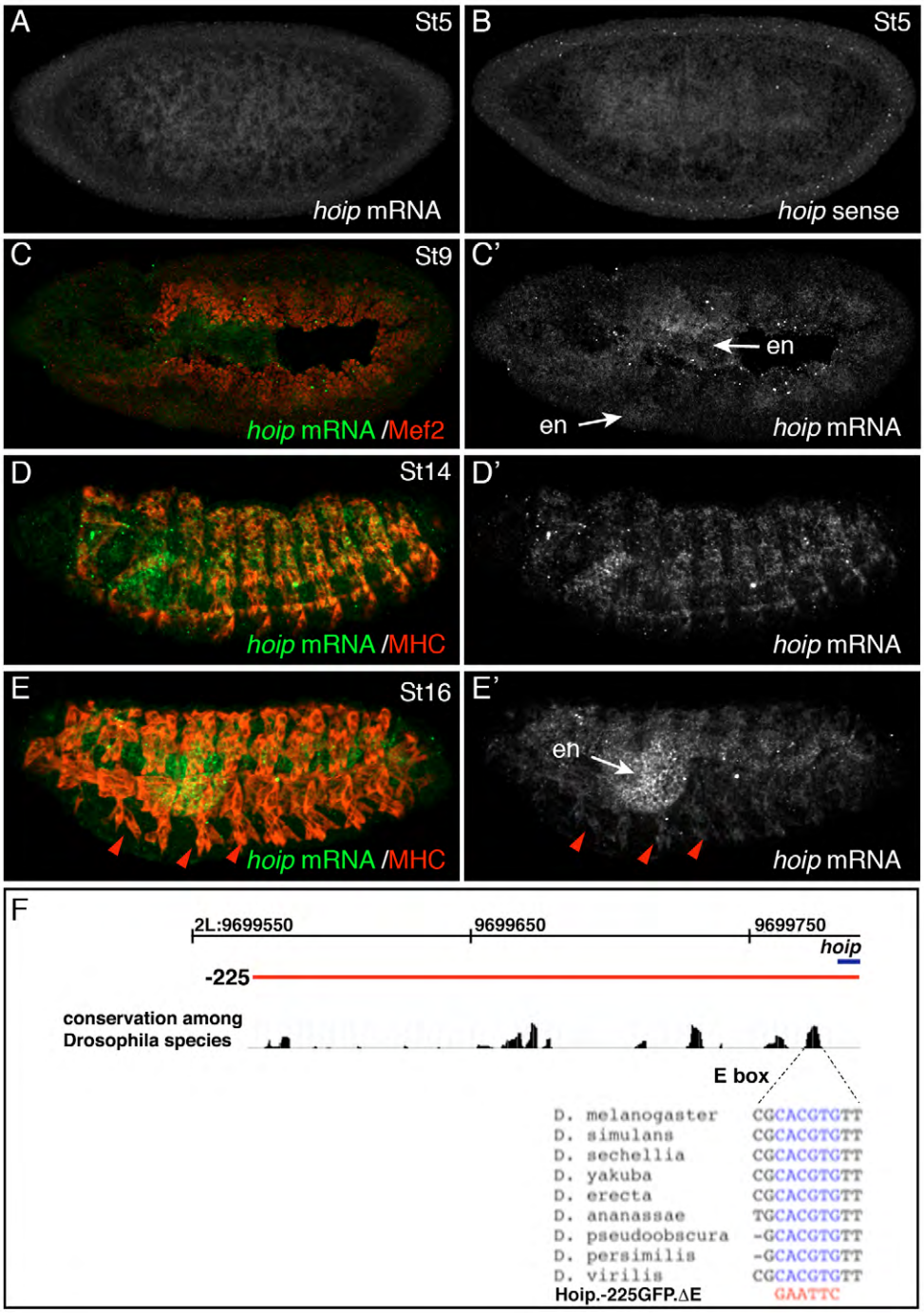


**Fig. S4. *hoip* expression during embryonic development.** (A-E) Wild-type embryos hybridized with RNA probes antisense (A,C-E) or sense (B) to the *hoip* mRNA. (**A**,**B**) Post-cellularization blastoderm embryos. Fluorescent intensity is comparable between the antisense and sense probes. (**C**) St9 embryo co-labeled for *hoip* (green) and Mef2 (red). Weak *hoip* expression has initiated in the endoderm and mesoderm. (**D**,**E**) St14 (D) and St16 (E) embryos co-labeled for *hoip* (green) and MHC (red). *hoip* is expressed at high levels in the endoderm (en) and at lower levels in the somatic musculature (red arrowheads). (**F**) Genomic conservation 225 bp 5′ to the *hoip* transcriptional start site. The highly conserved E-box sequence and mutations in Hoip.-225.ΔEGFP are shown. Genomic coordinates refer to base pair positions along chromosome 2L.

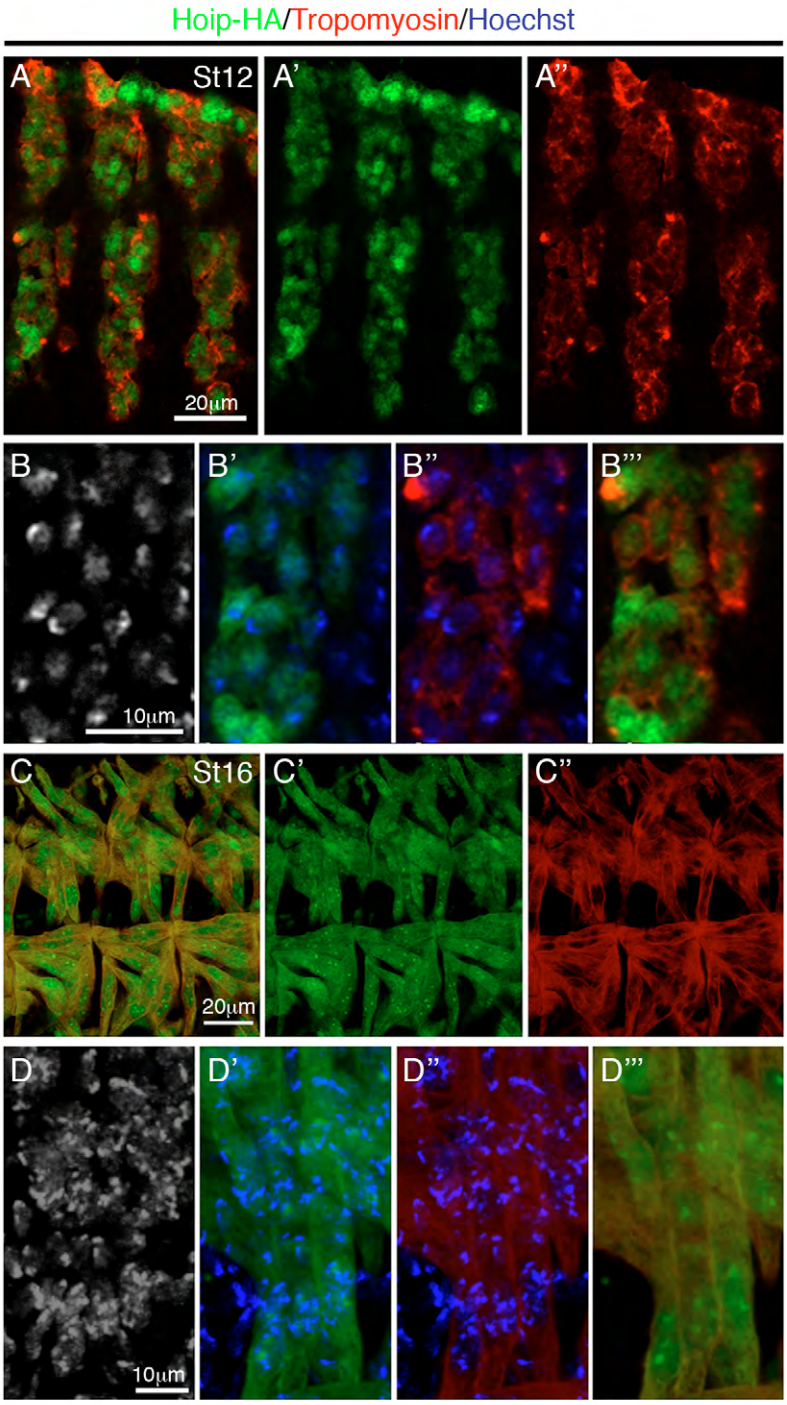


**Fig. S5. Hoip localizes to both the nucleus and the cytoplasm.** (A-D) Mef2>Hoip-HA embryos co-labeled for HA (green) and Tropomyosin (red). (**A**,**B**) Hoip is largely localized to the nucleus in St12 embryos, although some cytoplasmic staining is present. (**C**,**D**) Hoip is localized throughout the myofibers of St16 embryos. Enhanced localization is apparent in a subnuclear domain.

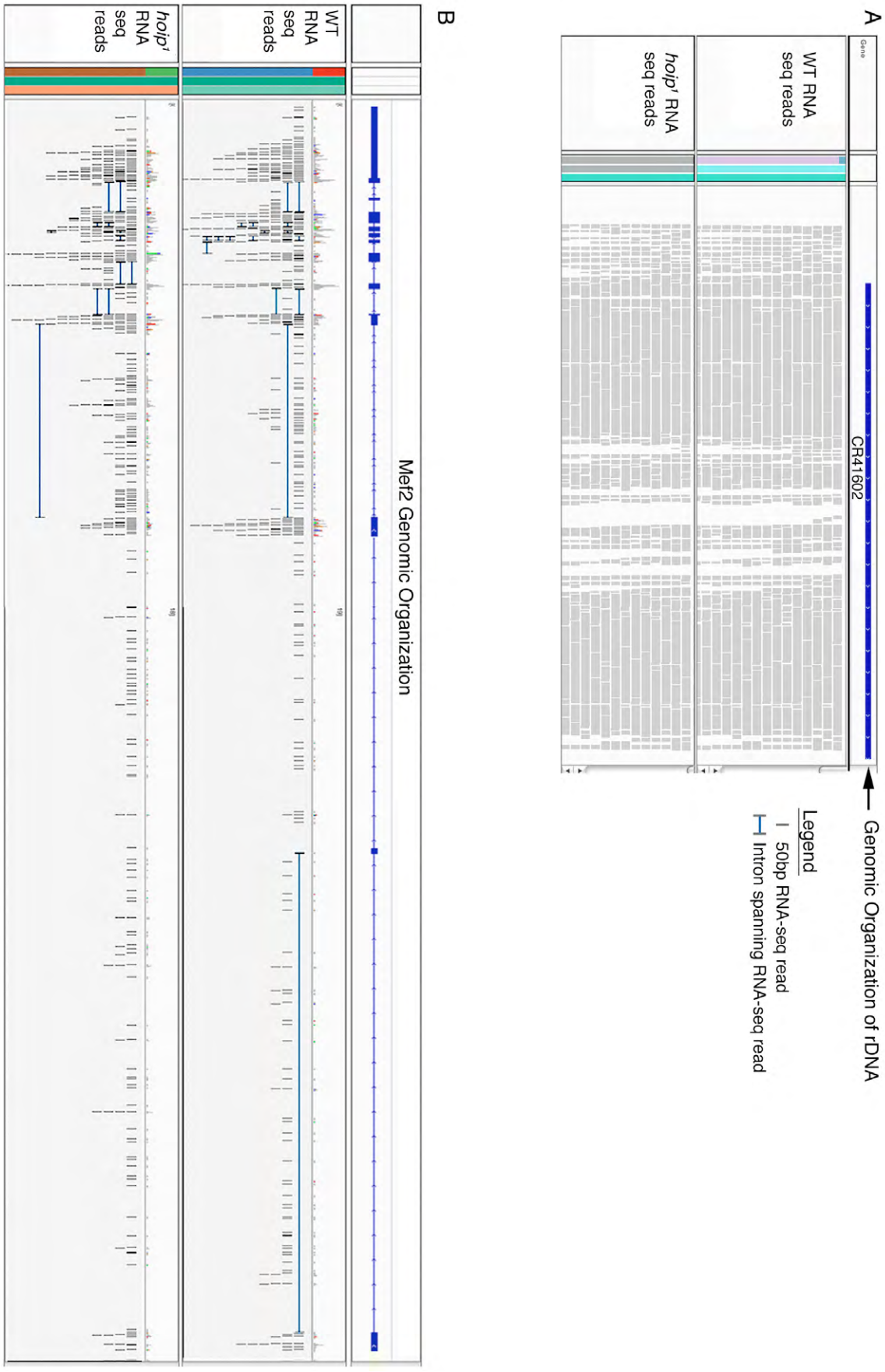


**Fig. S6. rRNA processing and *Mef2* expression are not affected in *hoip*$^{1}$ embryos.** (**A**,**B**) Screen shot from Integrative Genome Viewer at the rDNA locus (A; CR41602) and the Mef2 locus (B) showing RNA-seq reads from wild-type and *hoip*$^{1}$ embryos. Vertical grey bars represent a single sequencing read. Horizontal blue lines indicate a sequencing read across an intron. The number and positions of RNA-seq reads is comparable between genotypes at both loci.

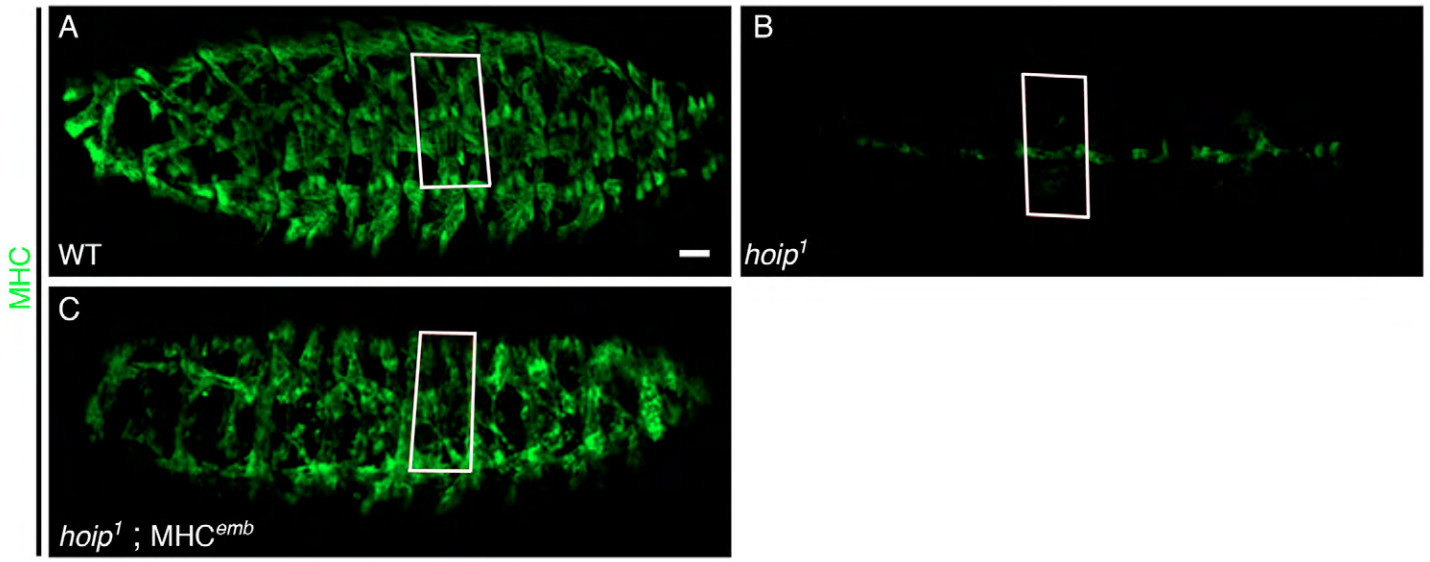


**Fig. S7. Method to quantify MHC expression by mean fluorescence intensity.** (**A-C**) Z-stacks including only the somatic muscles from St16 embryos stained for MHC. MHC expression was clearly restored in *hoip*$^{1}$ embryos by *MHC*$^{emb}$; however, muscle morphology was not (compare A with C). To quantify MHC expression in the somatic musculature (SM), we used the Zeiss LSM Zen 2011 software to trace the medial region of a segment using SBMs to define anterior-posterior position of each segment (white boxes). The software then calculated mean fluorescent intensity (MFI) within each boxed region. We also measured fluorescent intensity in the visceral musculature (VM). To normalize MHC expression, we divided SM MFI by VM MFI to obtain relative fluorescence for each segment.

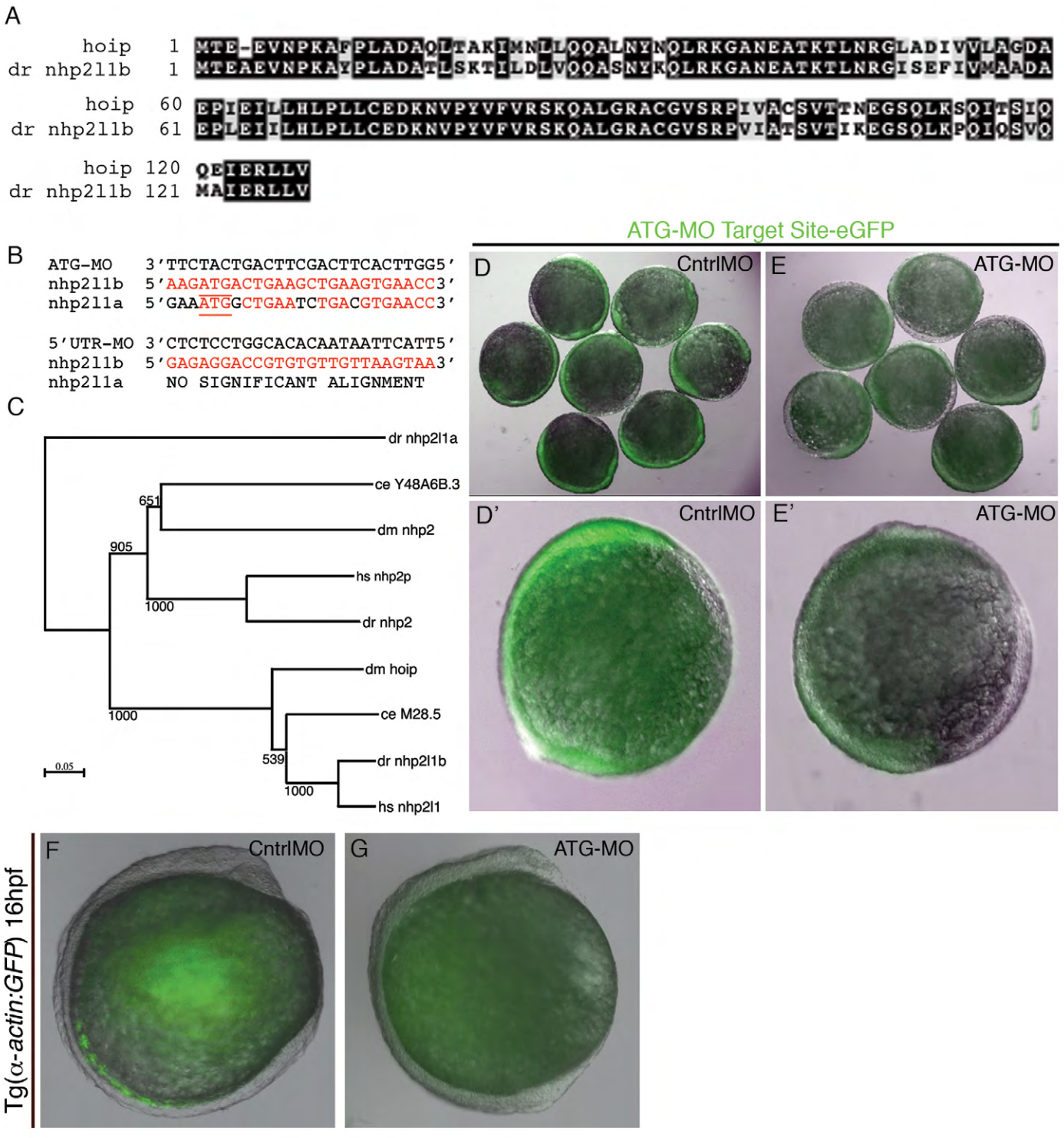


**Fig. S8. *nhp2l1b* is a Hoip orthologue and the *nhp2l1b* ATG-MO efficiently blocks translation.** (**A**) Alignment between Hoip and zebrafish *nhp2l1b* protein sequences. Identical amino acids are shaded black; similar amino acids are shaded gray. (**B**) Alignment of the *nhp2l1a/b* translational start sequences with the ATG-MO and 5'UTR-MO. Target nucleotides are red. The beginning of the ORF is underlined. (**C**) Phylogenetic analysis of NHP2 and NHP2L1 proteins in worms (ce), flies (dm), zebrafish (dr) and humans (hs). Bootstrap values are given. (**D**) Zebrafish embryos co-injected with Control-MO and an eGFP construct containing the *nhp2l1b* target site in the 5′UTR show robust eGFP expression at 12 hpf. (**E**) Embryos co-injected with ATG-MO and the same eGFP construct as in D show a significant reduction in eGFP expression. (**F**,**G**) Tg(α-*actin:GFP*) embryos injected with ATG-MO did not develop beyond 16 hpf.

**Table S1. Muscle development in *hoip* embryos**

| Muscle* | *DO1* | *DO2* | *DA 3* | *DO 3* | *DO 4* | *DO 5* | *LT1-4* | *DT 1* | *LO 1* | *SBM* | *VO 1-3* | *VA 1-2* |
|---|---|---|---|---|---|---|---|---|---|---|---|---|
| *hoip*$^{1}$ | 97 (36) | 94 (36) | 33 (36) | 13 (36) | 38 (36) | 19 (36) | 47 (144) | 91 (36) | 47 (36) | 94 (36) | 61 (90) | 64 (62) |
| *hoip*$^{1}$/ Df(2L)ED690 | 77 (31) | 100 (31) | 38 (31) | 16 (31) | 54 (31) | 32 (31) | 41 (124) | 93 (31) | 41 (31) | 67 (31) | 52 (93) | 77 (62) |
| *hoip*$^{1}$/*P{lacW}hoip*$^{K07104}$ | 100 (34) | 100 (34) | 53 (34) | 14 (34) | 44 (34) | 41 (34) | 33 (136) | 76 (34) | 50 (34) | 91 (34) | 71 (66) | 75 (48) |
| *P{lacW}hoip*$^{K07104}$ | 86 (22) | 78 (22) | 9 (22) | 0 (22) | 18 (22) | 18 (22) | 4 (88) | 36 (22) | 4 (22) | 59 (22) | 16 (66) | 23 (44) |

*Muscles extending across the segment scored positive

Data are percentage of positive muscles (number of muscles scored)

**Table S2. Differential gene expression in 6-10 hour *hoip*$^{1}$ embryos**

| Gene | Wild-type value | *hoip* value | Fold change | *P* value |
|---|---|---|---|---|
| abba | 25.7008 | 0.3275 | 0.01274 | 0.00002 |
| Acsl | 193.6320 | 82.4571 | 0.42584 | 0.00143 |
| Actn | 235.0040 | 103.6920 | 0.44124 | 0.00014 |
| Adh | 308.0260 | 45.7923 | 0.14866 | 0.00000 |
| Adk1 | 66.7169 | 5.9337 | 0.08894 | 0.00033 |
| Ahcy13 | 355.8390 | 152.4240 | 0.42835 | 0.00401 |
| alphaTub85E | 99.3420 | 25.6589 | 0.25829 | 0.00004 |
| arg | 285.5680 | 34.4369 | 0.12059 | 0.00445 |
| Atf6 | 184.9760 | 74.7937 | 0.40434 | 0.00113 |
| ATPsyn-g | 620.1150 | 296.6300 | 0.47835 | 0.00164 |
| betaTub97EF | 124.1460 | 13.9371 | 0.11226 | 0.00000 |

| | | | | |
|---|---|---|---|---|
| BM-40-SPARC | 197.7130 | 54.6709 | 0.27652 | 0.00022 |
| bt | 248.1740 | 13.6823 | 0.05513 | 0.00000 |
| Ca-alpha1D | 27.9455 | 10.2013 | 0.36505 | 0.00417 |
| Ca-beta | 24.3753 | 2.5030 | 0.10268 | 0.00062 |
| cals | 521.7950 | 248.3170 | 0.47589 | 0.00810 |
| CaMKI | 182.9920 | 64.2499 | 0.35111 | 0.00020 |
| CAP | 86.9704 | 36.7742 | 0.42284 | 0.00011 |
| Caps | 179.0760 | 75.8946 | 0.42381 | 0.00000 |
| Cda4 | 140.2440 | 65.9648 | 0.47036 | 0.00617 |
| Cf2 | 66.7754 | 20.9347 | 0.31351 | 0.00101 |
| CG10249 | 65.6698 | 27.0462 | 0.41185 | 0.00023 |
| CG10591 | 2167.7900 | 628.6480 | 0.29000 | 0.00000 |
| CG10625 | 96.9136 | 2.9092 | 0.03002 | 0.00000 |
| CG10737 | 142.7700 | 42.1398 | 0.29516 | 0.00000 |
| CG11155 | 26.3139 | 6.6147 | 0.25138 | 0.00258 |

| | | | | |
|---|---|---|---|---|
| CG11198 | 81.6923 | 31.6125 | 0.38697 | 0.00047 |
| CG11255 | 199.1450 | 88.5562 | 0.44468 | 0.00039 |
| CG11658 | 124.5830 | 58.0435 | 0.46590 | 0.00199 |
| CG11883 | 17.8655 | 1.6973 | 0.09500 | 0.00033 |
| CG12769 | 27.3271 | 8.2212 | 0.30084 | 0.00727 |
| CG13124 | 34.9772 | 12.4803 | 0.35681 | 0.00720 |
| CG13183 | 30.3052 | 5.5422 | 0.18288 | 0.00318 |
| CG13397 | 70.7670 | 21.9354 | 0.30997 | 0.00209 |
| CG13698 | 145.5600 | 53.7993 | 0.36960 | 0.00039 |
| CG14265 | 191.3600 | 0.0000 | 0.00000 | 0.00023 |
| CG14817 | 589.0110 | 97.1897 | 0.16500 | 0.00833 |
| CG14869 | 32.6878 | 11.2547 | 0.34431 | 0.00039 |
| CG15093 | 157.8800 | 12.2214 | 0.07741 | 0.00000 |
| CG15251 | 34.8088 | 1.9145 | 0.05500 | 0.00643 |
| CG15309 | 53.2676 | 15.7721 | 0.29609 | 0.00827 |

| | | | | |
|---|---|---|---|---|
| CG15618 | 29.7964 | 9.6678 | 0.32446 | 0.00003 |
| CG15822 | 45.2577 | 17.9422 | 0.39644 | 0.00026 |
| CG1607 | 68.4284 | 23.6532 | 0.34566 | 0.00357 |
| CG1674 | 104.1200 | 3.5355 | 0.03396 | 0.00001 |
| CG16884 | 156.7830 | 1.3108 | 0.00836 | 0.00000 |
| CG16885 | 247.5510 | 2.8119 | 0.01136 | 0.00004 |
| CG17549 | 104.3110 | 13.2131 | 0.12667 | 0.00017 |
| CG17598 | 164.8950 | 69.0480 | 0.41874 | 0.00311 |
| CG1764 | 62.8433 | 21.1004 | 0.33576 | 0.00455 |
| CG17816 | 34.8959 | 12.4392 | 0.35647 | 0.00207 |
| CG1824 | 81.5638 | 40.0639 | 0.49120 | 0.00400 |
| CG18522 | 38.5264 | 18.1660 | 0.47152 | 0.00566 |
| CG18661 | 32.8536 | 5.0490 | 0.15368 | 0.00362 |
| CG18675 | 15.8026 | 1.5630 | 0.09891 | 0.00653 |
| CG2219 | 143.0870 | 56.4341 | 0.39441 | 0.00381 |

| | | | | |
|---|---|---|---|---|
| CG2930 | 66.8025 | 6.7124 | 0.10048 | 0.00001 |
| CG2950 | 68.0822 | 34.2304 | 0.50278 | 0.00443 |
| CG2962 | 372.1370 | 100.6710 | 0.27052 | 0.00003 |
| CG30101 | 96.4232 | 11.8547 | 0.12294 | 0.00004 |
| CG3011 | 106.0890 | 34.2676 | 0.32301 | 0.00327 |
| CG30458 | 44.2715 | 0.7229 | 0.01633 | 0.00007 |
| CG30460 | 78.2668 | 31.4999 | 0.40247 | 0.00002 |
| CG31004 | 88.4885 | 17.5975 | 0.19887 | 0.00000 |
| CG31140 | 58.8638 | 19.0361 | 0.32339 | 0.00000 |
| CG31323 | 20.3243 | 1.9758 | 0.09721 | 0.00058 |
| CG3164 | 354.7930 | 173.0310 | 0.48769 | 0.00035 |
| CG31999 | 54.3378 | 10.3593 | 0.19064 | 0.00000 |
| CG32352 | 17.0136 | 1.9147 | 0.11254 | 0.00009 |
| CG32373 | 26.2502 | 3.7408 | 0.14250 | 0.00380 |
| CG32581 | 33.2508 | 2.7799 | 0.08360 | 0.00151 |

| | | | | |
|---|---|---|---|---|
| CG32813 | 97.8948 | 46.8468 | 0.47854 | 0.00294 |
| CG33144 | 47.1899 | 23.2984 | 0.49371 | 0.00270 |
| CG33205 | 151.1240 | 9.7741 | 0.06468 | 0.00000 |
| CG33977 | 733.7690 | 54.7722 | 0.07465 | 0.00085 |
| CG3588 | 54.3898 | 5.6839 | 0.10450 | 0.00001 |
| CG3793 | 69.7514 | 16.3636 | 0.23460 | 0.00510 |
| CG40263 | 77.1697 | 14.6049 | 0.18926 | 0.00005 |
| CG42326 | 24.2489 | 0.4969 | 0.02049 | 0.00018 |
| CG42492 | 84.9767 | 30.5867 | 0.35994 | 0.00000 |
| CG42527 | 185.2060 | 89.3761 | 0.48258 | 0.00129 |
| CG42533 | 45.7777 | 19.2573 | 0.42067 | 0.00501 |
| CG42673 | 77.4045 | 32.9339 | 0.42548 | 0.00614 |
| CG42741 | 20.4978 | 1.1266 | 0.05496 | 0.00641 |
| CG4467 | 40.2310 | 18.5803 | 0.46184 | 0.00049 |
| CG4562 | 34.0110 | 2.9619 | 0.08709 | 0.00001 |

| | | | | |
|---|---|---|---|---|
| CG4692 | 912.1890 | 414.2920 | 0.45417 | 0.00773 |
| CG4822 | 63.7431 | 15.4715 | 0.24272 | 0.00014 |
| CG5080 | 476.0120 | 126.7830 | 0.26634 | 0.00000 |
| CG5322 | 36.5403 | 7.3002 | 0.19978 | 0.00082 |
| CG5381 | 46.1005 | 12.6364 | 0.27411 | 0.00561 |
| CG5804 | 267.2140 | 0.0000 | 0.00000 | 0.00174 |
| CG5830 | 162.1450 | 80.2979 | 0.49522 | 0.00334 |
| CG5853 | 88.4155 | 26.1122 | 0.29533 | 0.00096 |
| CG5910 | 39.0743 | 3.5508 | 0.09087 | 0.00227 |
| CG5958 | 1026.3700 | 428.3170 | 0.41732 | 0.00144 |
| CG6043 | 32.5517 | 6.9578 | 0.21374 | 0.00032 |
| CG6388 | 92.7134 | 28.3814 | 0.30612 | 0.00301 |
| CG6672 | 151.9640 | 72.3595 | 0.47616 | 0.00080 |
| CG6972 | 86.6755 | 10.0643 | 0.11611 | 0.00012 |
| CG7203 | 103.2540 | 0.0000 | 0.00000 | 0.00001 |

| | | | | |
|---|---|---|---|---|
| CG7203 | 103.2540 | 0.0000 | 0.00000 | 0.00001 |
| CG7298 | 226.4770 | 2.8344 | 0.01252 | 0.00000 |
| CG7675 | 82.4901 | 34.9946 | 0.42423 | 0.00001 |
| CG7715 | 105.4550 | 0.0000 | 0.00000 | 0.00035 |
| CG7920 | 179.5330 | 61.1720 | 0.34073 | 0.00001 |
| CG7998 | 352.3630 | 75.3197 | 0.21376 | 0.00000 |
| CG8086 | 16.4205 | 4.7136 | 0.28705 | 0.00745 |
| CG8193 | 835.7910 | 220.8040 | 0.26419 | 0.00007 |
| CG8303 | 39.5537 | 12.0205 | 0.30390 | 0.00285 |
| CG8630 | 41.7814 | 1.5594 | 0.03732 | 0.00001 |
| CG9184 | 2626.3900 | 896.2130 | 0.34123 | 0.00000 |
| CG9331 | 163.9160 | 31.4306 | 0.19175 | 0.00010 |
| CG9380 | 101.9050 | 26.2261 | 0.25736 | 0.00000 |
| CG9416 | 159.5170 | 72.8624 | 0.45677 | 0.00637 |
| CG9527 | 52.0325 | 12.0834 | 0.23223 | 0.00155 |

| | | | | |
|---|---|---|---|---|
| CG9603 | 1277.9900 | 593.6690 | 0.46453 | 0.00003 |
| CG9619 | 23.3602 | 4.1184 | 0.17630 | 0.00006 |
| CG9743 | 121.2990 | 43.6324 | 0.35971 | 0.00018 |
| CG9747 | 109.8010 | 38.4442 | 0.35013 | 0.00073 |
| CG9850 | 16.3071 | 1.7034 | 0.10446 | 0.00034 |
| CG9990 | 38.8872 | 3.9755 | 0.10223 | 0.00001 |
| cher | 268.4920 | 90.8359 | 0.33832 | 0.00000 |
| chrb | 524.0690 | 248.8120 | 0.47477 | 0.00065 |
| Cht3 | 183.3590 | 39.5191 | 0.21553 | 0.00000 |
| Cpr62Bc | 73.4912 | 3.4134 | 0.04645 | 0.00006 |
| Cpr65Ea | 768.1140 | 33.2480 | 0.04329 | 0.00000 |
| cpx | 64.3182 | 14.6317 | 0.22749 | 0.00010 |
| CRMP | 86.8474 | 31.3974 | 0.36152 | 0.00227 |
| CYLD | 137.7420 | 46.6807 | 0.33890 | 0.00405 |
| Cyp309a2 | 51.1353 | 13.0595 | 0.25539 | 0.00027 |

| | | | | |
|---|---|---|---|---|
| deltaCOP | 280.8840 | 141.0960 | 0.50233 | 0.00001 |
| dpr7 | 45.0698 | 6.2485 | 0.13864 | 0.00272 |
| drpr | 80.2505 | 40.6775 | 0.50688 | 0.00000 |
| emp | 91.7095 | 23.7796 | 0.25929 | 0.00040 |
| Epac | 44.0771 | 13.2918 | 0.30156 | 0.00006 |
| eya | 64.8562 | 23.1432 | 0.35684 | 0.00510 |
| fau | 135.1110 | 0.0000 | 0.00000 | 0.00000 |
| fok | 231.0960 | 100.3170 | 0.43409 | 0.00547 |
| Gad1 | 24.8103 | 1.6205 | 0.06531 | 0.00002 |
| Galpha73B | 30.3547 | 0.9903 | 0.03262 | 0.00615 |
| Gasp | 1254.2300 | 379.6490 | 0.30270 | 0.00000 |
| Gel | 113.5200 | 36.9592 | 0.32557 | 0.00059 |
| Gfat1 | 112.0150 | 30.1142 | 0.26884 | 0.00008 |
| Gfat2 | 148.8290 | 67.0459 | 0.45049 | 0.00280 |
| Glut1 | 64.3970 | 25.5972 | 0.39749 | 0.00155 |

| | | | | |
|---|---|---|---|---|
| Got2 | 92.7271 | 24.2257 | 0.26126 | 0.00179 |
| Gpo-1 | 42.2637 | 4.4773 | 0.10594 | 0.00011 |
| grn | 103.0120 | 50.6430 | 0.49162 | 0.00188 |
| haf | 127.1860 | 60.3035 | 0.47414 | 0.00462 |
| ia2 | 24.9502 | 0.9657 | 0.03870 | 0.00000 |
| ImpL3 | 354.4180 | 65.5088 | 0.18484 | 0.00000 |
| iotaTry | 23222.1000 | 7344.8800 | 0.31629 | 0.00000 |
| kdn | 406.4710 | 191.7070 | 0.47164 | 0.00196 |
| l(2)01289 | 34.9121 | 1.5863 | 0.04544 | 0.00000 |
| l(2)03709 | 453.0830 | 212.6080 | 0.46925 | 0.00169 |
| l(2)efl | 139.5990 | 5.9545 | 0.04265 | 0.00003 |
| LamC | 181.5150 | 37.5050 | 0.20662 | 0.00000 |
| mas | 155.4540 | 60.9205 | 0.39189 | 0.00084 |
| mbl | 182.6290 | 86.3384 | 0.47275 | 0.00398 |
| Megalin | 194.0080 | 47.3070 | 0.24384 | 0.00000 |

| | | | | |
|---|---|---|---|---|
| Mf | 160.0220 | 1.6157 | 0.01010 | 0.00000 |
| Mhc | 726.6050 | 38.8825 | 0.05351 | 0.00000 |
| Mipp1 | 223.4110 | 112.1830 | 0.50214 | 0.00691 |
| Mlc1 | 837.2200 | 56.5194 | 0.06751 | 0.00000 |
| Mlc2 | 738.3910 | 68.5564 | 0.09285 | 0.00000 |
| Mob2 | 63.0313 | 25.5342 | 0.40510 | 0.00001 |
| Msp-300 | 156.9930 | 43.6981 | 0.27834 | 0.00000 |
| Msr-110 | 183.3070 | 40.4618 | 0.22073 | 0.00000 |
| mura | 149.8970 | 53.8473 | 0.35923 | 0.00007 |
| n-syb | 38.6363 | 3.4608 | 0.08957 | 0.00022 |
| Nckx30C | 18.8468 | 2.6763 | 0.14200 | 0.00002 |
| Nep2 | 121.8840 | 43.4931 | 0.35684 | 0.00157 |
| Nnf1a | 162.6400 | 45.1467 | 0.27759 | 0.00213 |
| Nurf-38 | 324.2540 | 155.6600 | 0.48005 | 0.00255 |
| Oatp33Ea | 44.0468 | 12.5061 | 0.28393 | 0.00338 |

| | | | | |
|---|---|---|---|---|
| Obp44a | 206.1100 | 0.0000 | 0.00000 | 0.00008 |
| obst-E | 62.6213 | 0.9349 | 0.01493 | 0.00005 |
| pgant3 | 67.1310 | 26.2108 | 0.39044 | 0.00028 |
| Pgm | 730.4410 | 149.3760 | 0.20450 | 0.00588 |
| Pif1A | 60.5008 | 21.7064 | 0.35878 | 0.00001 |
| PKD | 77.6680 | 24.3038 | 0.31292 | 0.00075 |
| PQBP-1 | 78.8846 | 38.2711 | 0.48515 | 0.00206 |
| ps | 360.4450 | 174.2810 | 0.48352 | 0.00000 |
| Rab-RP4 | 495.6050 | 62.7785 | 0.12667 | 0.00262 |
| Rab7 | 496.8930 | 236.2550 | 0.47546 | 0.00496 |
| Rbp6 | 68.6119 | 9.4344 | 0.13750 | 0.00001 |
| rec | 24.9292 | 6.0120 | 0.24116 | 0.00236 |
| RhoGAP100F | 38.6191 | 15.9435 | 0.41284 | 0.00011 |
| rut | 47.1320 | 20.9665 | 0.44485 | 0.00042 |
| Rya-r44F | 62.7417 | 27.0400 | 0.43097 | 0.00065 |

| | | | | |
|---|---|---|---|---|
| salm | 131.1010 | 62.0813 | 0.47354 | 0.00000 |
| scaf | 101.2600 | 16.3263 | 0.16123 | 0.00000 |
| SelG | 148.5730 | 47.7733 | 0.32155 | 0.00167 |
| serp | 422.5820 | 155.8250 | 0.36875 | 0.00000 |
| sgl | 271.7720 | 127.0570 | 0.46751 | 0.00501 |
| slo | 17.1657 | 4.4506 | 0.25927 | 0.00414 |
| Spn77Ba | 21.9980 | 1.1494 | 0.05225 | 0.00544 |
| Strn-Mlck | 25.6701 | 6.5128 | 0.25371 | 0.00000 |
| sv | 61.5652 | 26.8702 | 0.43645 | 0.00333 |
| synaptogyrin | 24.1509 | 2.5238 | 0.10450 | 0.00089 |
| Syt1 | 26.7950 | 7.0848 | 0.26441 | 0.00062 |
| Tace | 57.4618 | 16.9370 | 0.29475 | 0.00417 |
| TepII | 85.7617 | 36.8163 | 0.42929 | 0.00575 |
| Tina-1 | 376.2530 | 92.1554 | 0.24493 | 0.00006 |
| Tm1 | 1179.4600 | 590.3450 | 0.50052 | 0.00000 |

| | | | | |
|---|---|---|---|---|
| Tm2 | 236.8290 | 23.4468 | 0.09900 | 0.00000 |
| Tpi | 85.7148 | 26.3455 | 0.30736 | 0.00735 |
| TpnC47D | 1137.7500 | 43.3073 | 0.03806 | 0.00000 |
| TpnC73F | 310.8360 | 45.3916 | 0.14603 | 0.00000 |
| trol | 92.6705 | 14.6083 | 0.15764 | 0.00000 |
| Tsp42Ea | 98.0492 | 46.6541 | 0.47582 | 0.00832 |
| TwdlL | 187.6780 | 0.0000 | 0.00000 | 0.00000 |
| Uhg5 | 276.9450 | 101.8660 | 0.36782 | 0.00362 |
| Unc-89 | 17.9081 | 1.4018 | 0.07828 | 0.00000 |
| up | 496.6070 | 36.6903 | 0.07388 | 0.00000 |
| usnp | 239.4150 | 96.9262 | 0.40484 | 0.00781 |
| Vha13 | 599.8410 | 275.5040 | 0.45929 | 0.00003 |
| Vha68-1 | 82.3499 | 33.4698 | 0.40643 | 0.00045 |
| vig | 385.8230 | 153.7520 | 0.39851 | 0.00000 |
| vkg | 156.3580 | 31.1849 | 0.19945 | 0.00000 |

| | | | | |
|---|---|---|---|---|
| wupA | 387.3000 | 27.5334 | 0.07109 | 0.00000 |
| Zasp66 | 87.0525 | 1.1663 | 0.01340 | 0.00003 |
| Zn72D | 139.6570 | 57.0876 | 0.40877 | 0.00230 |
| zormin | 47.2647 | 10.4859 | 0.22185 | 0.00000 |
| Acph-1 | 43.4594 | 241.1100 | 5.54793 | 0.00000 |
| Aef1 | 146.4810 | 297.2880 | 2.02954 | 0.00478 |
| aPKC | 121.9500 | 279.3850 | 2.29097 | 0.00001 |
| Art1 | 242.4790 | 531.7740 | 2.19307 | 0.00118 |
| Ate1 | 39.0081 | 73.1226 | 1.87455 | 0.00308 |
| aub | 56.4823 | 98.7710 | 1.74871 | 0.00793 |
| ball | 171.4560 | 333.7020 | 1.94628 | 0.00034 |
| Bap60 | 421.5060 | 697.0230 | 1.65365 | 0.00036 |
| bcd | 63.8502 | 160.6040 | 2.51533 | 0.00078 |
| BicC | 27.4546 | 107.4950 | 3.91537 | 0.00001 |
| BicD | 111.1150 | 206.2440 | 1.85613 | 0.00057 |

| | | | | |
|---|---|---|---|---|
| borr | 313.7790 | 629.6920 | 2.00680 | 0.00021 |
| Bsg25D | 146.2920 | 276.9470 | 1.89311 | 0.00038 |
| BubR1 | 80.5678 | 180.9800 | 2.24630 | 0.00005 |
| bur | 180.8900 | 338.4700 | 1.87113 | 0.00121 |
| CG10083 | 102.4790 | 201.0980 | 1.96234 | 0.00012 |
| CG11164 | 76.2473 | 199.2020 | 2.61257 | 0.00722 |
| CG12391 | 161.1550 | 321.4480 | 1.99464 | 0.00737 |
| CG12734 | 73.7598 | 145.6700 | 1.97493 | 0.00006 |
| CG14435 | 36.5679 | 99.6366 | 2.72470 | 0.00030 |
| CG14764 | 163.1420 | 353.1810 | 2.16487 | 0.00004 |
| CG15141 | 163.9630 | 351.3140 | 2.14264 | 0.00609 |
| CG1518 | 247.8010 | 384.9000 | 1.55326 | 0.00167 |
| CG16970 | 4.5993 | 23.3453 | 5.07585 | 0.00528 |
| CG1962 | 198.9030 | 413.9530 | 2.08118 | 0.00175 |
| CG2051 | 205.5650 | 419.1920 | 2.03922 | 0.00818 |

| | | | | |
|---|---|---|---|---|
| CG2924 | 364.3240 | 729.1350 | 2.00133 | 0.00000 |
| CG2938 | 75.4931 | 176.2400 | 2.33451 | 0.00173 |
| CG30085 | 125.2360 | 343.5470 | 2.74318 | 0.00000 |
| CG30497 | 278.0410 | 538.4850 | 1.93671 | 0.00016 |
| CG31755 | 24.9920 | 69.3976 | 2.77679 | 0.00188 |
| CG31875 | 17.2983 | 103.0400 | 5.95669 | 0.00063 |
| CG3227 | 144.5160 | 332.4690 | 2.30057 | 0.00345 |
| CG32365 | 63.6367 | 164.4680 | 2.58449 | 0.00220 |
| CG3238 | 66.1893 | 193.1280 | 2.91780 | 0.00036 |
| CG33181 | 55.1074 | 139.6530 | 2.53420 | 0.00146 |
| CG42351 | 16.7495 | 62.3572 | 3.72293 | 0.00515 |
| CG42732 | 5.1984 | 16.5247 | 3.17884 | 0.00448 |
| CG4300 | 321.5820 | 670.3470 | 2.08453 | 0.00000 |
| CG4911 | 243.5320 | 419.8970 | 1.72420 | 0.00541 |
| CG5003 | 117.4080 | 221.5270 | 1.88682 | 0.00664 |

| | | | | |
|---|---|---|---|---|
| CG5098 | 51.4592 | 113.8990 | 2.21339 | 0.00398 |
| CG5568 | 22.7570 | 61.9223 | 2.72102 | 0.00439 |
| CG6051 | 128.0830 | 383.6580 | 2.99538 | 0.00000 |
| CG6241 | 55.6652 | 133.7950 | 2.40357 | 0.00432 |
| CG6425 | 43.2409 | 117.9910 | 2.72869 | 0.00411 |
| CG6461 | 30.9774 | 127.6630 | 4.12116 | 0.00000 |
| CG7357 | 89.1638 | 221.8540 | 2.48816 | 0.00419 |
| CG7433 | 115.4730 | 434.6690 | 3.76427 | 0.00000 |
| CG7824 | 64.8566 | 184.4170 | 2.84345 | 0.00450 |
| CG8116 | 154.2400 | 285.7130 | 1.85239 | 0.00471 |
| CG8173 | 159.6780 | 380.9250 | 2.38560 | 0.00012 |
| CG8177 | 123.7370 | 243.6640 | 1.96922 | 0.00000 |
| CG8290 | 73.7468 | 142.1180 | 1.92711 | 0.00721 |
| CG8944 | 109.7400 | 194.5750 | 1.77306 | 0.00573 |
| CG9062 | 82.6832 | 185.9320 | 2.24873 | 0.00020 |

| | | | | |
|---|---|---|---|---|
| CG9393 | 135.6090 | 303.3170 | 2.23671 | 0.00002 |
| chif | 171.8770 | 342.3200 | 1.99166 | 0.00000 |
| cnn | 178.3990 | 374.4030 | 2.09868 | 0.00095 |
| coro | 201.5780 | 359.2250 | 1.78206 | 0.00018 |
| Cpsf160 | 86.3761 | 182.3080 | 2.11064 | 0.00151 |
| crm | 101.2880 | 178.3820 | 1.76114 | 0.00168 |
| CycA | 552.3510 | 939.0740 | 1.70014 | 0.00003 |
| CycB | 1287.3700 | 2954.1100 | 2.29469 | 0.00023 |
| Edc3 | 114.6820 | 241.3340 | 2.10437 | 0.00226 |
| exu | 16.0356 | 63.6793 | 3.97110 | 0.00044 |
| fl(2)d | 200.3200 | 343.5310 | 1.71491 | 0.00055 |
| for | 168.6020 | 330.3640 | 1.95943 | 0.00352 |
| fs(2)ltoPP43 | 149.0240 | 291.3330 | 1.95493 | 0.00133 |
| G-ialpha65A | 322.3930 | 630.7580 | 1.95649 | 0.00003 |
| Gap69C | 131.7660 | 218.4400 | 1.65778 | 0.00320 |

| | | | | |
|---|---|---|---|---|
| hang | 222.0300 | 391.2560 | 1.76218 | 0.00346 |
| heix | 161.8620 | 264.4980 | 1.63410 | 0.00008 |
| HP5 | 146.5290 | 289.1320 | 1.97320 | 0.00474 |
| l(1)G0269 | 106.2820 | 165.2180 | 1.55453 | 0.00305 |
| Lk6 | 434.1760 | 776.2680 | 1.78791 | 0.00809 |
| LpR2 | 33.5198 | 78.2008 | 2.33297 | 0.00120 |
| Mapmodulin | 485.4570 | 951.0330 | 1.95905 | 0.00023 |
| mol | 116.6800 | 285.0380 | 2.44289 | 0.00000 |
| mrj | 201.0180 | 371.7790 | 1.84948 | 0.00130 |
| Msh6 | 27.7488 | 67.7988 | 2.44332 | 0.00697 |
| muskelin | 106.5290 | 340.6590 | 3.19780 | 0.00001 |
| ncd | 178.4470 | 379.7040 | 2.12783 | 0.00009 |
| Nlp | 1328.1400 | 2396.1700 | 1.80415 | 0.00820 |
| norpA | 13.8622 | 41.4837 | 2.99258 | 0.00265 |
| Not1 | 363.3890 | 603.0990 | 1.65965 | 0.00000 |

| | | | | |
|---|---|---|---|---|
| Nuf2 | 99.5041 | 183.2350 | 1.84148 | 0.00297 |
| Obp56a | 0.0000 | 161.2760 | und | 0.00157 |
| otu | 18.2523 | 56.1326 | 3.07537 | 0.00350 |
| PEK | 150.9750 | 288.4890 | 1.91084 | 0.00427 |
| Pink1 | 110.5080 | 203.3170 | 1.83983 | 0.00350 |
| Pmm45A | 111.6540 | 296.5350 | 2.65584 | 0.00034 |
| Poc1 | 81.7573 | 196.7340 | 2.40632 | 0.00711 |
| poe | 133.7730 | 214.7520 | 1.60534 | 0.00003 |
| proPO-A1 | 43.5178 | 222.5680 | 5.11442 | 0.00000 |
| ptip | 65.7316 | 118.5520 | 1.80357 | 0.00011 |
| ptr | 22.4477 | 43.1218 | 1.92099 | 0.00781 |
| Pxt | 26.5660 | 117.9900 | 4.44139 | 0.00003 |
| Rcd1 | 197.9670 | 319.0070 | 1.61142 | 0.00193 |
| RhoGAP54D | 30.3514 | 72.4985 | 2.38864 | 0.00750 |
| rig | 58.3268 | 108.5820 | 1.86161 | 0.00732 |

| | | | | |
|---|---|---|---|---|
| Ripalpha | 106.0340 | 392.3240 | 3.69996 | 0.00003 |
| RPA2 | 104.9070 | 372.4870 | 3.55067 | 0.00091 |
| RpII215 | 232.9340 | 372.1600 | 1.59771 | 0.00281 |
| Rpt4 | 327.0040 | 623.6410 | 1.90714 | 0.00051 |
| SMC2 | 96.7567 | 200.4190 | 2.07136 | 0.00005 |
| smg | 750.2190 | 2228.2500 | 2.97014 | 0.00000 |
| ssp3 | 47.9181 | 104.9210 | 2.18959 | 0.00326 |
| sti | 185.6460 | 353.5520 | 1.90444 | 0.00323 |
| Su(var)2-10 | 322.9430 | 560.4340 | 1.73540 | 0.00000 |
| Su(var)2-HP2 | 112.7700 | 207.5120 | 1.84013 | 0.00519 |
| Taf12 | 179.4620 | 399.9310 | 2.22851 | 0.00021 |
| thr | 115.3340 | 328.6780 | 2.84980 | 0.00001 |
| tlk | 246.1990 | 403.7060 | 1.63976 | 0.00001 |
| tor | 38.6324 | 94.7882 | 2.45360 | 0.00091 |
| Trf4-1 | 160.3040 | 315.3580 | 1.96725 | 0.00279 |

| | | | | |
|---|---|---|---|---|
| tum | 258.8920 | 528.6690 | 2.04205 | 0.00212 |
| twe | 138.3430 | 396.1770 | 2.86374 | 0.00000 |
| Uba2 | 244.0670 | 419.2780 | 1.71788 | 0.00008 |
| UbcD2 | 318.5530 | 673.5540 | 2.11442 | 0.00027 |
| Uch-L3 | 169.4910 | 324.7130 | 1.91581 | 0.00775 |
| Uev1A | 574.7470 | 923.3250 | 1.60649 | 0.00280 |
| Usp7 | 202.0050 | 337.6360 | 1.67142 | 0.00000 |
| vlc | 283.0970 | 505.1150 | 1.78425 | 0.00001 |
| wapl | 115.2550 | 253.6930 | 2.20115 | 0.00041 |
| wdn | 127.8800 | 229.4830 | 1.79452 | 0.00280 |
| yuri | 19.1355 | 71.9366 | 3.75932 | 0.00024 |

Downregulated transcripts are shaded red; upregulated transcripts are shaded green.

**Table S3. Differential isoform expression in 6-10hr *hoip*$^{1}$ embryos**

| Gene | Wild-type value | *hoip* value | Fold change | *P* value | Transcript defect |
|---|---|---|---|---|---|
| aub | 56.48230 | 98.77100 | 1.74871 | 0.00793 | Enhanced splicing |
| ptip | 65.73160 | 118.55200 | 1.80357 | 0.00011 | Enhanced splicing |
| sti | 185.64600 | 353.55200 | 1.90444 | 0.00323 | Enhanced splicing |
| CG8177 | 123.73700 | 243.66400 | 1.96922 | 0.00000 | Enhanced splicing |
| CG42748 | 175.85800 | 90.52090 | 0.51474 | 0.00432 | Exon inclusion |
| kcc | 89.84850 | 46.96120 | 0.52267 | 0.00085 | Exon inclusion |
| Ser | 84.99020 | 44.45880 | 0.52311 | 0.00064 | Exon inclusion |
| Ppn | 555.02200 | 306.51800 | 0.55226 | 0.00000 | Exon inclusion |
| Ca-P60A | 498.64100 | 275.82100 | 0.55315 | 0.00723 | Exon inclusion |
| CG32000 | 480.65000 | 268.36300 | 0.55834 | 0.00024 | Exon inclusion |
| hth | 835.08400 | 505.59300 | 0.60544 | 0.00059 | Exon inclusion |
| Mbs | 167.98500 | 107.22400 | 0.63830 | 0.00395 | Exon inclusion |

| | | | | | |
|---|---|---|---|---|---|
| tlk | 246.19900 | 403.70600 | 1.63976 | 0.00001 | Exon inclusion |
| Su(var)2-HP2 | 112.77000 | 207.51200 | 1.84013 | 0.00519 | Exon inclusion |
| rig | 58.32680 | 108.58200 | 1.86161 | 0.00732 | Exon inclusion |
| ptr | 22.44770 | 43.12180 | 1.92099 | 0.00781 | Exon inclusion |
| CG8290 | 73.74680 | 142.11800 | 1.92711 | 0.00721 | Exon inclusion |
| chif | 171.87700 | 342.32000 | 1.99166 | 0.00000 | Exon inclusion |
| bip2 | 311.99200 | 203.80600 | 0.65324 | 0.00047 | Exon skipping |
| Atpalpha | 619.91700 | 429.29900 | 0.69251 | 0.00385 | Exon skipping |
| dikar | 85.61790 | 120.58700 | 1.40843 | 0.00286 | Exon skipping |
| CG1518 | 247.80100 | 384.90000 | 1.55326 | 0.00167 | Exon skipping |
| Su(var)2-10 | 322.94300 | 560.43400 | 1.73540 | 0.00000 | Exon skipping |
| vlc | 283.09700 | 505.11500 | 1.78425 | 0.00001 | Exon skipping |
| Ate1 | 39.00810 | 73.12260 | 1.87455 | 0.00308 | Exon skipping |
| for | 168.60200 | 330.36400 | 1.95943 | 0.00352 | Exon skipping |

| | | | | | |
|---|---|---|---|---|---|
| shot | 177.77600 | 112.71300 | 0.63401 | 0.00722 | Exon skipping/exon inclusion |
| mrj | 201.01800 | 371.77900 | 1.84948 | 0.00130 | Exon skipping/exon inclusion |
| sano | 95.19750 | 52.42650 | 0.55071 | 0.00662 | Exon skipping/inclusion |
| CG34417 | 31.43320 | 16.63610 | 0.52925 | 0.00058 | No splicing |
| mrt | 79.34430 | 42.20550 | 0.53193 | 0.00438 | No splicing |
| sm | 266.06100 | 135.89400 | 0.51076 | 0.00830 | Reduced splicing |
| crol | 319.13200 | 169.49200 | 0.53110 | 0.00000 | Reduced splicing |
| fz2 | 300.78100 | 160.47500 | 0.53353 | 0.00062 | Reduced splicing |
| if | 86.65180 | 48.43270 | 0.55893 | 0.00119 | Reduced splicing |
| VhaSFD | 325.35600 | 182.20800 | 0.56003 | 0.00003 | Reduced splicing |
| CG14425, Sxl | 368.62100 | 209.39300 | 0.56804 | 0.00010 | Reduced splicing |
| CG14767 | 311.92900 | 178.67400 | 0.57280 | 0.00070 | Reduced splicing |
| PNUTS | 187.48500 | 107.55800 | 0.57369 | 0.00145 | Reduced splicing |
| Pdp1 | 154.50300 | 89.82400 | 0.58137 | 0.00835 | Reduced splicing |

| | | | | | |
|---|---|---|---|---|---|
| A2bp1 | 203.49100 | 118.55600 | 0.58261 | 0.00818 | Reduced splicing |
| ct | 94.26300 | 56.17210 | 0.59591 | 0.00489 | Reduced splicing |
| rictor | 83.02180 | 49.61840 | 0.59766 | 0.00072 | Reduced splicing |
| nkd | 215.54700 | 130.30700 | 0.60454 | 0.00083 | Reduced splicing |
| Cirl | 438.24000 | 271.95700 | 0.62057 | 0.00068 | Reduced splicing |
| par-1 | 190.83200 | 124.93800 | 0.65470 | 0.00019 | Reduced splicing |
| Aats-glupro | 212.19200 | 140.44800 | 0.66189 | 0.00034 | Reduced splicing |
| grh | 178.67900 | 123.00500 | 0.68841 | 0.00292 | Reduced splicing |
| Rcd1 | 197.96700 | 319.00700 | 1.61142 | 0.00193 | Reduced splicing |
| hang | 222.03000 | 391.25600 | 1.76218 | 0.00346 | Reduced splicing |
| Nlp | 1328.14000 | 2396.17000 | 1.80415 | 0.00820 | Reduced splicing |
| fs(2)ltoPP43 | 149.02400 | 291.33300 | 1.95493 | 0.00133 | Reduced splicing |
| G-ialpha65A | 322.39300 | 630.75800 | 1.95649 | 0.00003 | Reduced splicing |

| | | | | | |
|---|---|---|---|---|---|
| cpo | 180.11500 | 105.18600 | 0.58399 | 0.00013 | Reduced splicing/exon inclusion |
| Pvr | 126.49100 | 75.74530 | 0.59882 | 0.00122 | Reduced splicing/exon inclusion |
| Eip75B | 341.18800 | 207.52200 | 0.60823 | 0.00418 | Reduced splicing/exon skipping |
| l(3)82Fd | 159.89400 | 100.41200 | 0.62799 | 0.00255 | Reduced splicing/exon skipping |
| Imp | 551.30400 | 374.13400 | 0.67863 | 0.00303 | Reduced splicing/exon skipping |
| Dscam | 147.12600 | 112.67700 | 0.76585 | 0.00043 | Reduced splicing/exon skipping |

**Table S4. Muscle elongation, target recognition and attachment mRNA expression in *hoip*$^{1}$ embryos**

| Gene | Muscle function | Fold change in *hoip*$^{1}$ embryos* | Stage of muscle phenotype | Reference |
|---|---|---|---|---|
| *Dynein heavy chain 64C* | Elongation | NC | Stage 15 | (Folker et al., 2012) |
| *pavarotti* | Elongation | NC | Stage 16 | (Guerin and Kramer, 2009) |
| *tumbleweed* | Elongation | 2.04 | Stage 14/15 | (Guerin and Kramer, 2009) |
| *derailed* | Recognition | NC | Stage 14 | (Callahan et al., 1996) |
| *echinoid* | Recognition | NC | Stage 16 | (Swan et al., 2006) |
| *kon-tiki* | Recognition | NC | Stage 13 | (Schnorrer et al., 2007) |
| *MSP-300* | Recognition | 0.27 | Stage 16 | (Rosenberg-Hasson et al., 1996) |
| *perdido* | Recognition | NC | Stage 13 | (Estrada et al., 2007) |
| *roundabout* | Recognition | NC | Stage 14 | (Steigemann et al., 2004) |
| *Slit* | Recognition | 0.66 | Stage 14 | (Steigemann et al., 2004) |
| *Stripe* | Recognition/ | NC | Stage 14 | (Frommer et al., 1996) |

| | | | | |
|---|---|---|---|---|
| | attachment | | | |
| *Glutamate Receptor Binding Protein* | Attachment | NC | Stage 13 | (Estrada et al., 2007) |
| *inflated* | Attachment | 0.56 | Stage 17 | (Bloor and Brown, 1998) |
| *Leucine-rich tendon-specific protein* | Attachment | NC | Stage 16 | (Wayburn and Volk, 2009) |
| *mind bomb 2* | Attachment | NC | Stage 15 | (Carrasco-Rando and Ruiz-Gomez, 2008) |
| *multiple edematous wings* | Attachment | NC | Stage 16 | (Chanana et al., 2007) |
| *myospheroid* | Attachment | NC | Stage 16 | (Brown, 1994) |
| *rhea* | Attachment | NC | Stage 16 | (Brown et al., 2002) |
| *slowdown* | Attachment | NC | Stage 16 | (Gilsohn and Volk, 2010a) |
| *Thrombospondin* | Attachment | NC | Stage 16 | (Subramanian et al., 2007) |
| *Tiggrin* | Attachment | NC | Stage 16/17 | (Bunch et al., 1998) |
| *vein* | Attachment | NC | Stage 16 | (Yarnitzky et al., 1998) |

*Fold change compared with wild-type embryos

**Table S5. Possible muscle elongation regulators misexpressed in *hoip*$^{1}$ embryos**

| Gene | Molecular function | Fold change in *hoip*$^{1}$ embryos |
|---|---|---|
| *Gelsolin* | Actin binding | 0.32 |
| *Rab7* | GTPase | 0.13 |
| *Rab18* | GTPase | 0.48 |
| *RhoGAP54D* | Rho GAP | 2.30 |
| *RhoGAP100F* | Rho GAP | 0.41 |
| *Tetraspanin 42Ea* | Transmembrane protein | 0.48 |
| *Unc-89* | Rho GEF | 0.07 |

**Table S6. Primer sequences**

| Primer | Forward primer | Reverse primer |
|---|---|---|
| **Site-directed mutagenesis** | | |
| *hoip*[1] | ATCAACTGCGCAAGGAAGCCAACGAGGCCAC | GTGGCCTCGTTGGCTTCCTTGCGCAGTTGAT |
| Hoip.-225.GFP* | TCTAGAACTCGCGGATGCGC | GGTACCAAGTGCTTTAAAATGCAACCTCTC |
| Hoip.-225ΔE.GFP | TTTCTAACGCTAACGGAATTCTTTGAAAGCGATTTC | GAAATCGCTTTCAAAGAATTCCGTTAGCGTTAGAAA |
| **qPCR** | | |
| *if* | CGATCCTTCCCACGAGATTA | GCAGTGGATTCTACGGCAAT |
| *Mf* | TCCAAAGCAGGTTGTCATTG | GCCACTCGGTATCTTTGAGC |
| *MHC* | CTGTTCAAGTGGCTGGTGAA | AATGGGTGTTGGTCAGCTTC |
| *Mlc2* | CAGCAACTGGGTGAAGTTGA | CAGCCAGAGATTCAGTGTGC |
| *Tm2* | CAGCTGACCAACCAGTTGAA | AAATCGTCGCAGATTGCTTT |
| *TpnC 47D* | TTTATTCAAGCCTCGGGTGT | CAGTCGTTAGCGGTGATCG |
| *TpnC 73F* | CAACAGCTTCGATCACCAGA | AAGTGGGTGGTGTTTTCCAG |
| *smyhc1* | GAGGAACCAGCAGAGAGTGG | CAGATTGTTGCGTCTCTCCA |
| *smyhc3* | TGGAGAGACGCAACAATCTG | CTGCCTCCTCAACCTCAGTC |

| | | |
|---|---|---|
| *tpma* | CCCGTAAGCTGGTGATTGTT | ACGAGTCTCAGCCTCCTTCA |
| *tpm2* | TGCAGATGCTCAAACTGGAC | TTGAGCGCGATCTAACTCCT |
| *Mef2a* | GGCTCTCCAGGGCTCTCTAT | CATCGTAGGAGGAGCAGGAG |
| *Mef2d* | GAGAATGCTCAGCGGTTAGG | TGTTGCCAAGTGGTCATGTT |
| *notch1* | CGAGCCCTTGTCATTATGGT | TCGCAGACACACTCATAGCC |
| *GAPDH* | GATACACGGAGCACCAGGTT | AACAGCAAAGGGGTCACATC |
| *Rpl32* | TTACTCGTTCTCTTGAGAACGC | CTTCAAGATGACCATCCGC |

*The PCR product was digested with Kpn/*Eco*RI to generate the Hoip.-225 fragment